Arabian Journal of Geosciences (2026) 19:120
https://doi.org/10.1007/s12517-026-12518-z

ORIGINAL PAPER

Assessing the impacts of cyclone 'Remal' induced storm surges on soil and water salinization in a coastal region of Bangladesh

Taposhi Habiba[1] · Alim Miah[1,2] · Tajim Ahammad[1] · Khairul Haque[1]

Received: 24 April 2025 / Accepted: 10 May 2026

Abstract
The southwestern coastal region of Bangladesh experienced severe environmental disruption due to Cyclone 'Remal'-induced storm surges, intensifying salinity stress in soil and freshwater systems. The study provides a post-cyclone evaluation of salinization in Sarankhola combining field and laboratory data, geospatial analysis, multivariate analysis, and indices obtained through satellite analyses to measure the extent and spatial variability of the salinity effect. Water quality analysis showed extensive saline intrusion, with average electrical conductivity of 3,273 µS/cm and peak values reaching 10,021 µS/cm, accompanied by elevated chloride (Cl^-, 4250 mg/l) and Total Dissolved Solids (TDS, 6500 mg/l); 13 times higher than WHO's guideline. Salinity in the soils was widespread, and the average EC was 3,481 µS/cm, with a maximum of 8,486 µS/cm. The disruption of biogeochemical processes was evident from excessive nutrient enrichment, as soil nitrogen (N) and phosphorus (P) concentrations reached 599 mg/kg and 936 mg/kg, respectively. Principal component analysis (PCA) showed salinity parameters (EC, TDS, Na^+, Cl^-) explained 83.7% of water variance, while soil salinity and nutrients accounted for 70.8% of variance. Satellite-based indicators derived from Sentinel-2 imagery, including the Normalized Difference Vegetation Index (NDVI), Normalized Difference Salinity Index (NDSI), and Soil Salinity Index (SI-ASTER), revealed vegetation loss of 104 km², a 50% expansion of high-salinity water zones, and a 17.6% rise in very highly saline soils. The results demonstrate that cyclone-induced storm surges act as a reinforcing mechanism for salinity persistence rather than transient disturbances, providing spatially explicit insights to support coastal management, embankment planning, disaster preparedness, and climate adaptation in vulnerable deltaic regions.

Keywords Cyclone 'Remal' · NDVI · NDSI · Salinization · Storm surges

Introduction

Coastal lands around the world are confronted with the challenge of low-lying land being exposed to both storm surges and saltwater intrusion due to tropical cyclones. Bangladesh's vast, low-lying terrain and long coastline make it vulnerable to severe storm surges caused by cyclones. Storm surges carrying salty coastal water into low-lying habitats severely degrade freshwater resources and agricultural land. Soil and water salinization are two major problems in the coastal regions of Bangladesh. Excessive water and soil salinization result in serious long-term environmental issues in coastal and deltaic locations, notably in heavily populated tropical deltas. Increased soil salinity hinders plant and crop growth, exacerbates soil sterility, and leads to poor seed germination (Mukherjee and Siddique 2022). Salinity adversely affects other income-generating activities such as pottery by rendering saline clay unsuitable for ceramics (Saha 2017). Salinized water also introduces toxic ions, severely impacting households that rely on freshwater ponds for irrigation and fishing (Mukherjee and Siddique 2022). Understanding the impacts of cyclones on salinization is crucial for mitigating adverse effects on livelihoods and ecosystems in Bangladesh. Bangladesh's coastal regions are vulnerable to various natural hazards because of their nearly leveled terrain and strategic location at the mouth

Responsible Editor: Biswajeet Pradhan.

✉ Alim Miah
alimbau31@gmail.com

[1] Department of Environmental Science and Engineering, Jatiya Kabi Kazi Nazrul Islam University, Trishal, Mymensingh 2224, Bangladesh

[2] Department of Environmental Science, Bangladesh Agricultural University, Mymensingh 2202, Bangladesh

Published online: 08 June 2026

of the "funnel-shaped" Bay of Bengal (Baten et al. 2015). The devastation caused by Cyclone 'Remal,' which struck Bangladesh in May 2024, underscores the vulnerability of these regions. Cyclone 'Remal' caused storm surges that destroyed freshwater and agricultural resources, collapsed embankments, and flooded large areas, forcing thousands of people to leave their homes (Bangladesh Meteorological Department 2024; IFRC 2024; Hossen et al. 2025). Storm surges triggered by Cyclone 'Remal' severely destroyed the sanitation infrastructure and water sources in the impacted districts (IFRC 2024; Hossen et al. 2025). Sundarbans, the largest mangrove forest in the world, suffered significant damage to its flora and fauna, adding to the long-term ecological strain. Cyclone 'Remal' caused Tk 722.17 crore in losses to Khulna's shrimp sector, and its long-term consequences on soil, water quality, and livelihoods are still unresolved and require further study (Hossain 2024). In recent research, similar trends of topography and water salinization in the post-cyclonic aftermaths of major cyclones in Bangladesh, including Sidr and Amphan, have been reported, showing that their effects are long-term on crop and freshwater productions (Hoque et al. 2016; Akhter et al. 2024). These results align with the trends found in this study, and hence there is a need to include spatially explicit assessment and mitigation analysis. However, despite various studies conducted to explore the effects of cyclones and related water and soil salinization processes, there is still no detailed spatial study combining remote sensing and geographic information systems (GIS) to measure the changes in soil and water salinities in the aftermath of significant cyclone events. Furthermore, available literature is relatively rarely able to evaluate the effectiveness of post-cyclone mitigation response measures, which constitutes a significant gap in the understanding of long-term resilience processes. The specified gaps limit the ability to create specific interventions to support the coastal areas in Bangladesh, hence making this study necessary and timely. The research aims to assess the impact of storm surges caused by Cyclone 'Remal' on soil and water salinization and evaluate the subsequent effects on agriculture and freshwater resources in a coastal region of Bangladesh. It seeks to develop spatial maps to assess salinization levels in soil and water post-cyclones and to identify mitigation strategies to evaluate their effectiveness in reducing the impacts of salinization in the study area. To address long-term effects, this study will use remote sensing, field sampling, and GIS analysis to gather longitudinal data, ensuring a thorough evaluation of salinization trends over time. Besides the research gap on the effectiveness of the existing mitigation strategies in reducing soil and water salinization after cyclone strikes, one of the hypotheses of this research is that the effective role of storm surges induced by Cyclone 'Remal' resulted in the severe salinization of the soil and water, causing a decline in the agricultural productivity and freshwater supply of the post-cyclone coasts. In contrast to the previous cyclone salinity studies on major cyclones such as SIDR, AILA, AMPHAN, and YAAS, which concentrated on either field sampling or remote sensing indices, the current study employs a hybrid approach that combines Sentinel-2–derived salinity and vegetation indices (NDVI, NDSI and SI-ASTER), GIS-based spatial analysis, and empirically calibrated EC measurements. The above integration across multiple disciplines enables high-resolution mapping and strict validation of salinity distributions, making it affordable to undertake a more thorough evaluation of the processes of cyclone-induced salinization and its resulting ecological impacts. Unlike previous studies, the study also evaluates the effectiveness of mitigation interventions after cyclones by putting salinization paths in relation to agricultural production and the accessibility of freshwater resources. Such contributions provide practical information applicable to resilience planning for vulnerable coastal communities.

Materials & methods

Study area

Sarankhola Upazila, a sub-district of Bagerhat district in Bangladesh, is the study area (between 22°13'–22°24' N and 89°46'–89°54' E). This area was largely devastated by severe cyclone 'Remal' (on 26 May 2024), also developed as the most expensive tropical cyclone recorded in Bangladesh for May 2024. It was the first cyclonic storm and depression of the North Indian Ocean cyclone season of 2024. At the southernmost point of the Bagerhat district, four unions make up Sarankhola Upazila. Located on the banks of the Baleshwar River and in the foothills of the Sundarbans, near the mouth of the Bay of Bengal, this coastal upazila is highly vulnerable to cyclones. The Baleshwar and Bhola rivers' influence causes the study area to be open to the sea and susceptible to wave and river activity, even though there are mangroves bordering some of its southern boundary (Nadiruzzaman and Paul 2013).

In addition, there are a lot of natural and physical resources in the area that are susceptible to harm from storm surges, flooding, and severe winds (Hoque et al. 2016). As this study has been conducted based on both qualitative and quantitative analysis, the detailed map of the study is given here. The field study was conducted in Sarankhola Upazila's four unions, shown in Fig. 1(b). The whole Sarankhola Upazila has been studied for the Remote Sensing method, shown in Fig. 1(a).

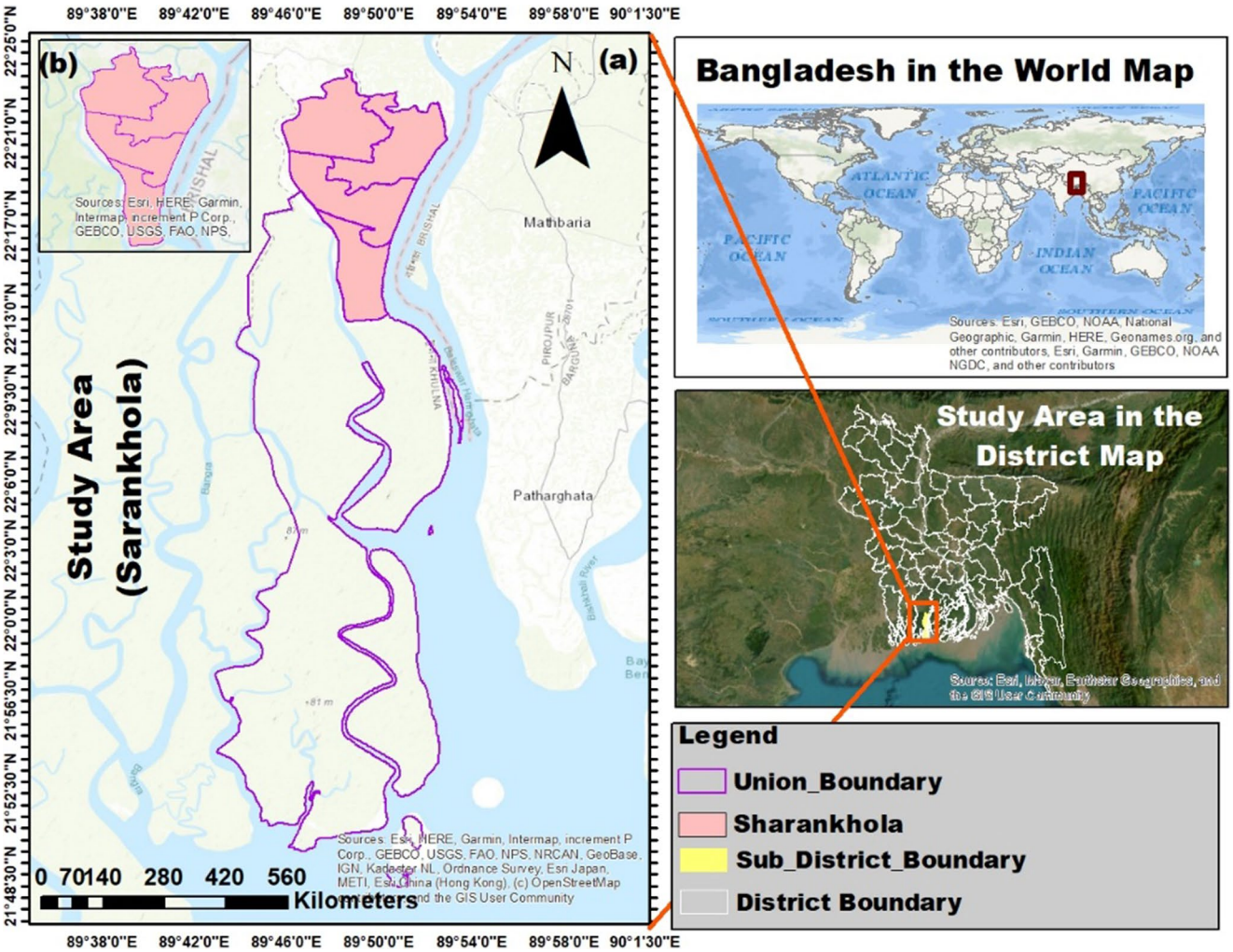

Fig. 1 Study area, Sarankhola Upazila under Bagerhat district in Bangladesh **(a)** Sarankhola Upazila & **(b)** four inter-coastal Unions of Sarankhola Upazila

Cyclone 'Remal'

The most recent severe storm, 'Remal' (pronounced Re-Mal), struck Bangladesh and West Bengal in May 2024. It was a tropical storm of moderate intensity and fatality. The Bangladesh Meteorological Department reports that on the evening of May 25, it evolved from a deep depression into a cyclone. The Oman word for 'sand' is where the term 'Remal' originated (The Indian Express 2024). On the evening of May 25, it strengthened from a deep depression into a cyclone (Bangladesh Meteorological Department 2024). At 8:30 p.m. on May 26, the cyclone made landfall as a strong storm on Sagar Island in the Sundarbans Delta of West Bengal (Fig. 2).

Soil and water sampling

Soil and water samples were collected between the 8th and 12th of October, 2024 at the four unions. This timeframe was chosen to measure salinity levels after the monsoon when cyclone-induced salt intrusion most likely persists. Water samples were collected in 20% nitric acid-equipped bottles soaked overnight and then rinsed with deionized water to avoid contamination. Sample bottles were sealed right after collection to avoid exposure to air.

In order to be reliable and representative, a combination of three subsamples collected within a 5-meter radius on each soil and water sampling point and later homogenized to create a composite sample was used. The pH, EC, and TDS were measured in situ in duplicate using a calibrated multiparameter meter (Hanna HI98194). The calibration of the instruments was performed before every sampling session. Quality assurance measures included the repeated measurement of 10% of samples, addition of reagent blanks, and testing with standard solutions to confirm accuracy of instruments. The determination of sodium (Na^+), chloride (Cl^-), and bicarbonate (HCO_3^-) was done

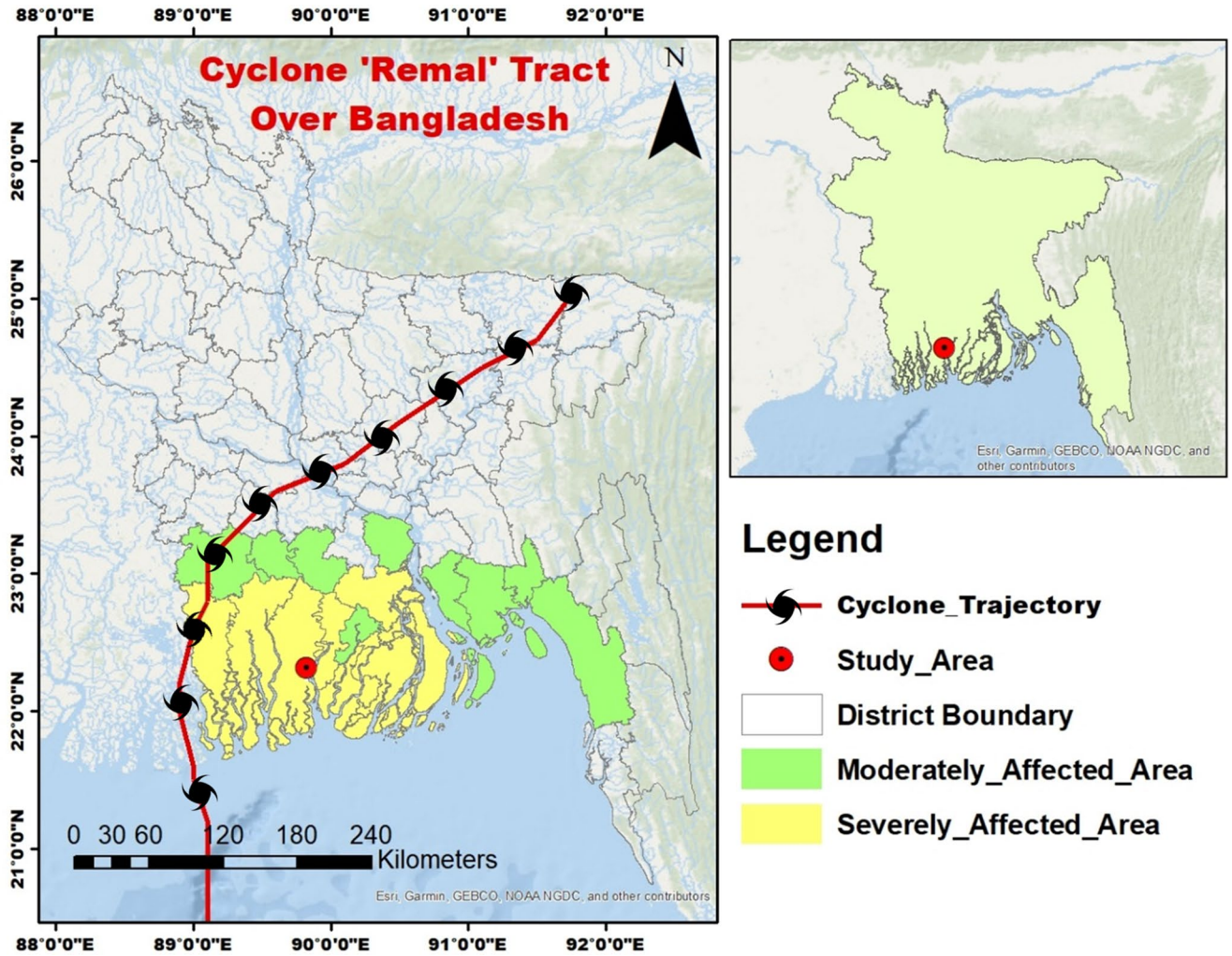

Fig. 2 Cyclone 'Remal' (2024) trajectory and affected areas

in the laboratory according to the protocols of the Department of Public Health and Engineering (DPHE), including duplicates and calibration standards to maintain the analytical precision.

Twelve soil samples were collected from riverbanks, ponds, and agricultural fields across four unions of Sarankhola Upazila (Dhansagar, Khantakata, Rayenda, and Southkhali) using a hand auger at a depth of 10–15 cm. The soil multi-sensor (One-Stop IoT Provider) was standardized for calibration and cleaning, after which in situ soil analyses were conducted for soil pH, EC, total nitrogen (N), potassium (K), and phosphorus (P). Samples were then sent to the Geochemistry Laboratory of ESE, JKKNIU, where the samples were kept in dry, clean, and cool places. The sample size (12 soil samples and 12 water samples) is quite small; nevertheless, it was established by the small geographical scope of the research area and the available resources. Systematic sampling was used to achieve spatial representativeness by using consistent intervals, as is done in other studies of cyclone impacts. Table 1 shows the locations and land use data for the soil samples, whereas Table 2. shows the data for the water samples, and the spatial map of the collection sites is shown in Fig. 3 below.

Table 1 Water sampling points with GPS coordinates

Union	Sampling ID	Geographical location	
		Latitude	Longitude
Dhansagar	**WS-1**	22.339	89.792
	WS-2	22.349	89.769
	WS-3	22.379	89.807
Khantakata	**WS-4**	22.348	89.871
	WS-5	22.364	89.855
	WS-6	22.329	89.834
Rayenda	**WS-7**	22.305	89.799
	WS-8	22.322	89.856
	WS-9	22.271	89.831
Southkhali	**WS-10**	22.257	89.829
	WS-11	22.233	89.811
	WS-12	22.272	89.808

Table 2 Soil sampling points with GPS coordinates

Union	Sampling ID	Geographical location	
		Latitude	Longitude
Dhansagar	**SS-1**	22.339	89.792
	SS-2	22.349	89.769
	SS-3	22.379	89.807
Khantakata	**SS-4**	22.348	89.871
	SS-5	22.364	89.855
	SS-6	22.329	89.834
Rayenda	**SS-7**	22.305	89.799
	SS-8	22.307	89.852
	SS-9	22.271	89.831
Southkhali	**SS-10**	22.257	89.829
	SS-11	22.233	89.811
	SS-12	22.272	89.808

Soil and water sample analysis

Standard procedures were used to analyze the main chemical components of soil and water and their quality aspects. Parameters such as soil temperature, pH, EC, N, P, and K were measured with a soil multi-sensor. Excel and SPSS were used to analyze the data for correlation checks and visualization. ArcGIS was used to create spatial distribution maps.

After collecting, water samples were taken to the central laboratories of the Department of Public Health Engineering to test the Cl^- and $HCO3^-$. Titrimetric analysis was used to measure the bicarbonate and Cl^- concentrations of the water samples.

HCO_3^- concentration was determined via titration using 0.1 N hydrochloric acid (HCl). The reaction follows:

$$HCO_3^- + HCl\ H_2CO_3\ +\ Cl^-$$

$$H_2CO_3\ H_2O + CO_2$$

The HCO_3^- concentration was calculated as

$$S_{[HCO_3^-]} = \frac{V_{HCI} \times\ S_{HCI}}{V_{Sample}}$$

Cl^- concentration was measured via titration with 0.1 N silver nitrate ($AgNO_3$), forming a white precipitate of silver chloride (AgCl). The reaction follows:

$$Ag^+\ + Cl^-\ AgCl$$

Cl^- concentration was calculated as

$$S_{[Cl^-]} = \frac{V_{AgNO_3} \times\ S_{AgNO_3}}{V_{Sample}}$$

The concentration of Na^+ was determined using flame atomic absorption spectroscopy (AAS) at 589.0 nm. Standard calibration was performed using Na^+ solutions of 1 mg/l, 5 mg/l, and 10 mg/l. Turbid samples were filtered before analysis. Absorbance was measured and converted

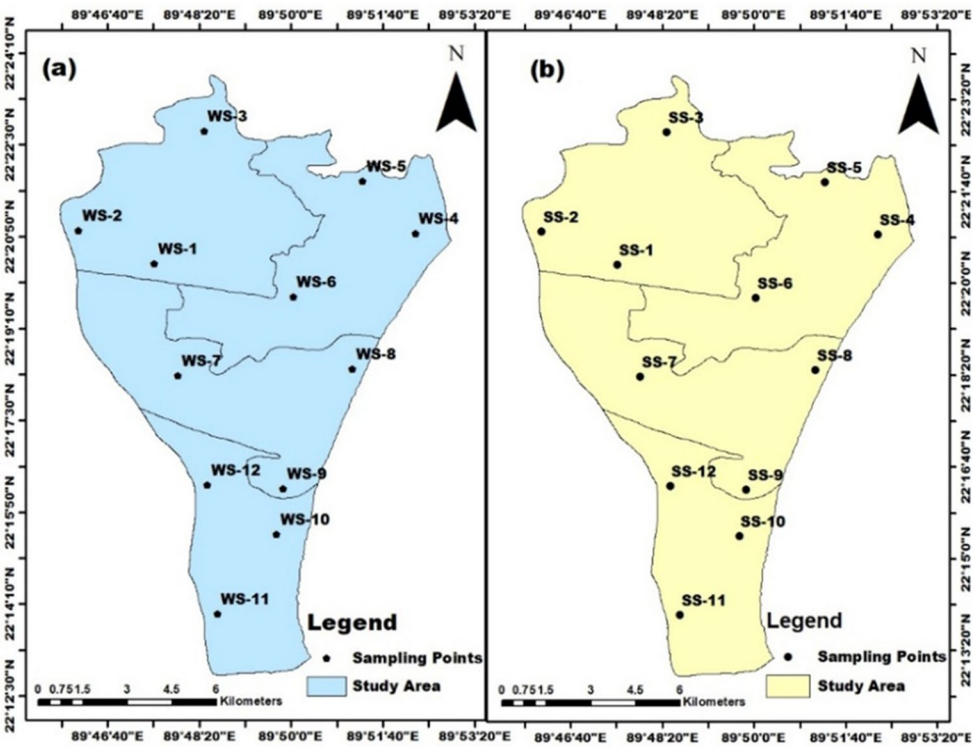

Fig. 3 Spatial map of sampling points; **(a)** Water sampling points, **(b)** Soil sampling points

into Na^+ concentration using the calibration curve. The final Na^+ concentration was calculated as.

$$Na^{+}Concentration(mg/l) = Measured\ Concentration \times Diluted\ Factor$$

Statistical analysis

Using IBM SPSS 25, the findings of the soil and water samples were analyzed using Pearson's correlation coefficient. By considering the covariance and the standard variations within the two data sets, Pearson's correlation coefficient, a linear correlation model, generates a value, r. This is the formula for calculating the standard Pearson's Correlation:

$$r := \frac{\Sigma\,(x_i - \overline{x})\,(y_i - \overline{y})}{\sqrt{\Sigma\,(x_i - \overline{x})^2\,\Sigma\,(y_i - \overline{y})^2}}$$

Unless otherwise indicated, Microsoft Excel 19 was used for most of the calculations.

Principal component analysis (PCA)

Principal Component Analysis (PCA) was used as a technique of dimensional reduction, as well as to determine the most influential factors in water and soil quality in the cyclone-affected region. PCA is a multivariate method used to reduce the number of variables in a certain dataset into a smaller collection of components that are uncorrelated, yet they maintain most of the variance within their dataset.

To ensure the comparison of the measurements, all variables were standardized (mean = 0, standard deviation = 1). This analysis was based on the correlation, and the components whose eigenvalues exceeded one were kept as stipulated by the Kaiser criterion (Ahamad et al. 2020). The suitability of the number of components was also supported through the Scree test. To implement the PCA, R (Version: 2025.09.2+418) was used, and the resulting component structure was shown in biplots showing the variable loading and sample clustering. In the case of the water samples, the variables that were used included pH, EC, TDS, HCO_3^-, Cl^-, and Na^+, and for soil samples, the variables included pH, EC, temperature, N, P and K.

The Principal Component Scores (PCS) are derived from a normalized data matrix Z of dimensions N × n, with each row representing an individual case i and each column corresponding to a variable j. Each entry z_{ij} denotes a value for a physical or derived variable.

Each observation z_{ij} can be represented as

$$Z_{ij} = \sum_{m=1}^{r} f_{im}\, a_{mj}$$

Where:

f_{im} = score of observation i on component m.

a_{mj} = loading of component m on variable j.

r = number of retained components (≤n).

The standardized data matrix Z (with n variables and N observations) can be expressed as:

$$Z = FA^T$$

Where:

F= matrix of PC scores.

A= matrix of loadings.

Satellite data analysis

Sentinel-2 imagery (10 m resolution) acquired from the Copernicus Open Access Hub was used to assess pre- and post-cyclone conditions. To ensure a precise representation of salinity intrusion and terrain changes brought on by the cyclone, these images were chosen based on surge conditions, proximity to the cyclone event, and the cloud cover. Two images (May 16 and June 7, 2024) were selected based on minimal cloud cover (Table 3).

The images were prepared using tools from ArcMap 10.8. The study area's shapefile was taken from Bangladesh's administrative map. The shapefile and composite picture were transformed into the same projection system, UTM ZONE WGS 1984.

NDVI calculation & image classification

NDVI measures vegetation health using near-infrared (NIR) and visible red (R) reflectance:

$$\mathrm{NDVI} = \frac{\mathrm{NIR} - \mathrm{RED}}{\mathrm{NIR} + \mathrm{RED}}$$

For Sentinel-2, the formula looks like this:

$$\mathrm{NDVI} = \frac{\mathrm{B8} - \mathrm{B4}}{\mathrm{B8} + \mathrm{B4}}$$

Table 3 Information of satellite image datasets

SI No	Satellite	Instrument	Image type	Processing Level	Acquisition Date	Spatial Resolution (m)	Cloud Coverage (%)
01	Sentinel-2	MSI	Multi-spectral	Level 2 A	16 May, 2024	10	15.008
02	Sentinel-2	MSI	Multi-spectral	Level 2 A	7 June, 2024	10	16.63

Here, B8 = Near Infrared light; B4 = Visible Red light. NDVI values help classify land cover types (as shown in Table 4).

NDSI calculation & image classification identifies soil salinity using Red and NIR bands:

$$\mathrm{NDSI} = \frac{\mathrm{RED} - \mathrm{NIR}}{\mathrm{RED} + \mathrm{NIR}}$$

For Sentinel-2, the formula looks like this:

$$\mathrm{NDSI} = \frac{\mathrm{B4} - \mathrm{B8}}{\mathrm{B4} + \mathrm{B8}}$$

Here, B4 = Visible Red Light; B8 = Near Infrared Red. NDSI ranges are used to classify soil salinity levels (as shown in Table 5).

SI_ASTER calculation & image classification

The SI_ASTER index, originally developed with ASTER imagery, was later adapted for use with Sentinel-2 to take advantage of its higher spatial resolution (10–20 m) and frequent revisit period, features that are important when monitoring post-cyclones in small areas of coastline. Sentinel-2 also provides Short-Wave Infrared (SWIR) and Near-Infrared (NIR) spectral bands, namely Band 11 (SWIR) and Band 8 (NIR), which have spectral features that are similar to ASTER, and thus allow effective application of the SI_ASTER formalism.

SI_ASTER (Soil Salinity Index) utilizes ASTER bands sensitive to soil salt content:

The formula used to determine the Study Area's SI_ASTER is as follows:

$$\mathrm{SI\_ASTER} = \frac{\mathrm{SWIR}_1 - \mathrm{SWIR}_2}{\mathrm{SWIR}_1 + \mathrm{SWIR}_2}$$

Table 4 NDVI values

Class	NDVI values
Water/Snow/Cloud	−1-0
Barren Land/Built-up/Rock	−0.2
Vegetation	0.2–1

Source: (Alex et al. 2017)

Table 5 Feature classes according to NDSI ranges

Class	NDSI Ranges
No Salinity	<0
Very Low Salinity	0–0.2
Low Salinity	0.2–0.4
Moderate Salinity	0.4–0.6
High Salinity	>0.6

Source: (Gerardo and De Lima 2022)

For Sentinel-2, the formula looks like this:

$$\mathrm{NDSI} = \frac{\mathrm{B11} - \mathrm{B12}}{\mathrm{B11} + \mathrm{B12}}$$

Here, B11 = Shortwave Infrared ($SWIR_1$); B12 = Shortwave Infrared ($SWIR_2$).

The classifications of salinity in soil and water were based on the existing standards and previous studies about salinity on the coast (Hoque et al. 2016; Mukherjee and Siddique 2022; Akter et al. 2025). In the case of soil, the EC values less than 4 dS/m were considered as non-saline, 4 to 8 dS/m as moderately saline, and 8 dS/m and above as highly saline. In the case of water, EC values less than 2 dS/m were considered fresh, values between 2 and 4 dS/m as slightly saline, and values beyond 4 S/m as highly saline. This was used to apply these thresholds to remote-sensing-obtained salinity indices (SI_ASTER, NDSI) and compare them to in-situ EC measurements collected in the field through field sampling (as shown in Table 6). Since in this research the conductivities were first measured in µS/cm, they were then converted to dS/m to allow some consistency with the accepted classification limits. The validation was done by comparing the classified salinity zones with ground EC readings that showed good concordance, therefore establishing the reliability of the classification methodology.

Area calculation

The reclassify tool in ArcMap 10.8 was used to carry out the reclassification. The following formula was used to get the feature area because the resolution of the image was 10 pixels; thus, the cell size was 10 m:

$$Feature\ Area = \{\{10 \times 10 \times (Count)\} \div (1000 \times 1000)\}\ sq.km$$

This methodological framework generated accurate and reliable results in evaluating soil and water quality attributes. It enables spatial assessment of the salinity distribution and changes in vegetation cover after cyclone 'Remal,' which provided critical information regarding its induced salinization (as shown in Fig. 4).

Table 6 Feature classes according to SI_ASTER ranges

Class	NDSI Ranges
Non-Saline	<−1.0-0.1
Slightly Saline	0.1–0.3
Moderately Saline	0.3–0.5
Highly Saline	0.5–0.7
Very Highly Saline	>0.7

Source: (Gerardo and De Lima 2022)

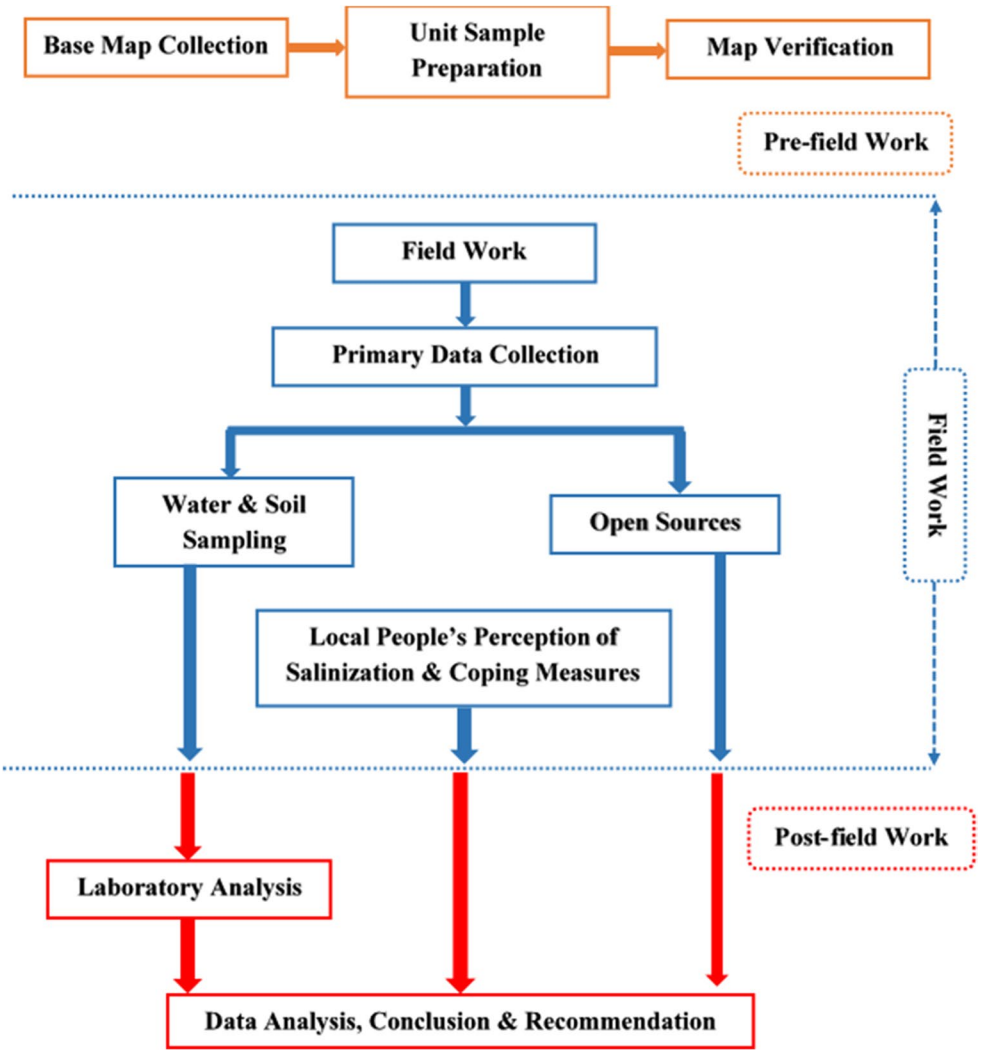

Fig. 4 Materials and methods flowchart of the study

Result

Water salinization

Water salinity is influenced by various dissolved salts present in water. The dissolved salts cause salinity, resulting from natural processes like seawater encroachment due to cyclonic storm surges (Ashrafuzzaman et al. 2022). To assess water salinity, water samples were tested for parameters contributing to salinity and compared with standard values. Key physicochemical parameters include pH, EC, TDS, temperature, Cl^-, HCO_3^-, Na^+, etc. The salinity of the water measurements from Supplementary Table 1 has been summarized here to make it clear. On the whole, the ECs of the soil were in the range of 306 to 10,021 µS/cm of the soil, with more than 60% of the samples being found to be moderate to highly saline. The water TDS ranges were in the range of 170 to 6,500 ppm, which indicated high intrusion of salinity in infested water. In the worst affected locations, Na^+ was detected up to 5,040 mg/l and Cl^- up to 4,000 mg/l, which is way beyond the WHO and ECR regulations. The results of the spatial analysis indicated that Southkhali and Khantakata were the most important salinity hotspots, with relatively lower values observed in Dhansagar. The full datasets are presented in Supplementary Table 1.

Physicochemical parameters

pH

pH measures the hydrogen ion concentration, indicating water's acidity or alkalinity. The optimal pH range for drinking water is 6.5–8.5 (ECR, 2023 and WHO). Our study found that 58% of the samples were within this range (Fig. 5). Some samples were slightly acidic, with the lowest pH recorded at 6.31. The average pH was 6.73, which is 3.8% lower than the lower WHO limit of 6.5, and 42% of the samples fell outside the recommended range.

Water with a pH of less than 6.5 can damage aquatic ecosystems, lower crop yields, and impact drinking water

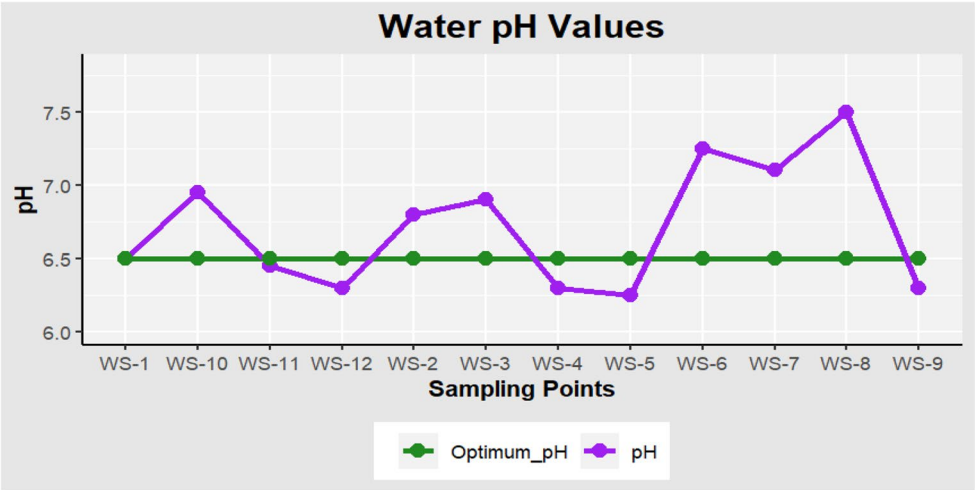

Fig. 5 A line chart of pH values of water samples with optimum pH

quality (Miah et al. 2024). The pH of water found in the study area was almost in the optimum range except for 5 samples. The possible causes of the mild acidity (pH < 6.5) could be organic matter breakdown, seawater intrusion, or acidic substances introduced by post-cyclone run-off.

TDS

The total concentration of dissolved ions (metals, salts, and minerals) in water is measured by TDS, expressed in mg/l or ppm. High TDS affects water taste and influences aquatic organisms' health and spawning conditions. Figure 6 shows a spatial map of the study area with TDS values found at each sampling point. According to the map, it is clear that the red marking zone governing WS-11 (6200 mg/l) and WS-12 (6500 mg/l) has a very high concentration of TDS available. The highest TDS concentration (6,500 mg/l) was 13 times greater than the recommendation of the World Health Organization (WHO) (500 mg/l); the overall mean TDS concentration (1,984.6 mg/l) was 297% above the limit. The average TDS was 1,984.6 mg/l, indicating saline intrusion in some areas, particularly in Southkhali Union, as shown by the red marking zone on the spatial map. According to a study that examined Landsat 8 imagery from 2014 to 2018, there was a notable increase in salinity levels after cyclones, with a 28.9% decrease in water areas with TDS levels between 100 and 600 mg/l and a 32.7% increase in places with TDS levels above 1200 mg/l (Ferdous et al. 2019). There are no major industrial sources in the study area, so the range of TDS values in some samples with high levels is probably due to soil erosion, organic matter breakdown, and seawater intrusion, not industrial activity. High TDS reduces crop yield by increasing osmotic stress and makes water unsuitable for freshwater fish breeding (Dasgupta et al. 2015).

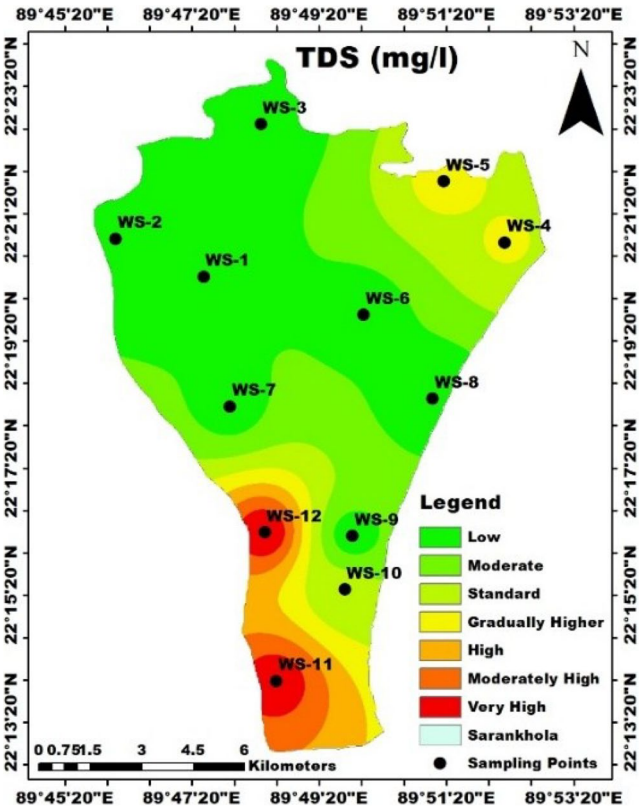

Fig. 6 Spatial map for TDS (mg/l) availability of water in study area

EC

The amount of dissolved salts in water is known as salinity, and it is commonly measured in parts per thousand (ppt) or EC in µS/cm. The concentration of dissolved ions determines conductivity; higher salt concentrations result in higher conductivity, which indicates salinity level. Figure 7 shows the overall spatial changes in water salinity. WS-12

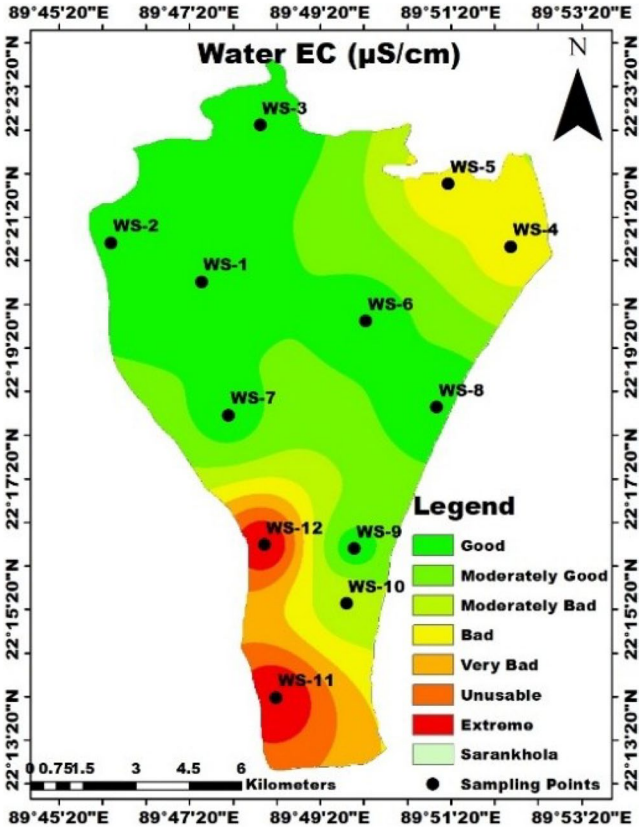

Fig. 7 Spatial map for water EC (µs/cm) availability in study area

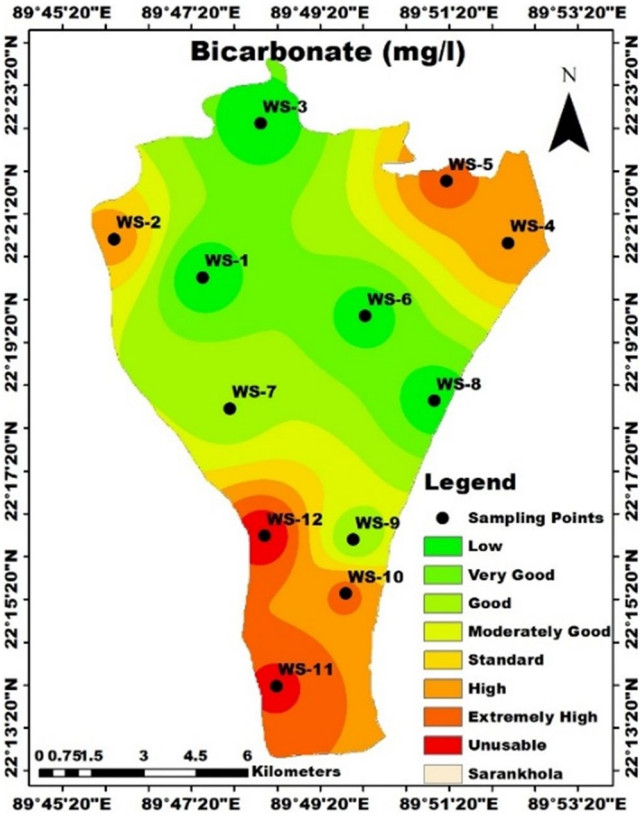

Fig. 8 Spatial map for HCO_3^- (mg/l) availability of water in study area

had the highest EC of 10,021 µS/cm, whereas WS-11, WS-4, and WS-5 also had notable values.

The average EC of 3273 µS/cm was recorded, highlighting severe salinity in Southkhali and parts of Khontakata. This amount represents a 118% increase compared to the safe irrigation threshold (1,500 µS/cm). High salinity significantly impacts crops, soil quality, and drinking water, creating water scarcity. A study of surface water salinity during 2001–2005 and 2006–2010 revealed that cyclones Sidr (2007) and Aila (2009) increased surface water salinity (EC > 1,500 µS/cm) in southwestern coastal Bangladesh, moving the freshwater contour 11–28 km northward and 4–22 km eastward (Haq et al. 2024). High EC impacts crop growth by inducing osmotic stress, reducing water uptake, and degrading soil structure, while also harming freshwater fish spawning (Tsai et al. 2024). Increased salinity is indicated by elevated EC values in Southkhali and Khontakata, most likely due to their proximity to the shore rather than industrial activity, as no industrial zone has been found.

HCO_3^- concentration

HCO_3^- concentration can impact water alkalinity and soil sodicity. A few samples (WS-2, WS-4, WS-10, WS-11, and WS-12) exceeded WHO guidelines (Fig. 8). High HCO_3^- levels are probably caused by saltwater intrusion as a contributing factor. Saltwater brings dissolved salts when intrudes into freshwater sources. It contains HCO_3^-, although its concentration is lower than that of Cl^- or Na^+. The complex reaction between freshwater and saltwater might be the reason behind the increasing concentration of HCO_3^-. If the highly concentrated HCO_3^- water is used for irrigation purposes, it can lead to soil sodicity, which means the presence of a high proportion of Na^+ ions. According to research evaluating the water quality of coastal rivers, 67% of sampling sites had HCO_3^- concentrations above acceptable levels throughout the pre-monsoon and post-monsoon seasons (Uddin et al. 2024). As agricultural activities have been detected in Khontakata, increased HCO_3^- levels may be the consequence of fertilizer and irrigation use; in Southkhali, however, they are most likely the consequence of seawater intrusion, the breakdown of carbonate minerals, and decreased freshwater inflow.

Cl^- concentration

Most water bodies naturally contain Cl^- ions, one of the main anions in salt water, which are produced when rocks and soil minerals dissolve. The elevated concentration of Cl^- represented in Fig. 9 suggests that the water samples from WS-4, WS-5, WS-6, WS-10, WS-11, and WS-12 have high concentrations of

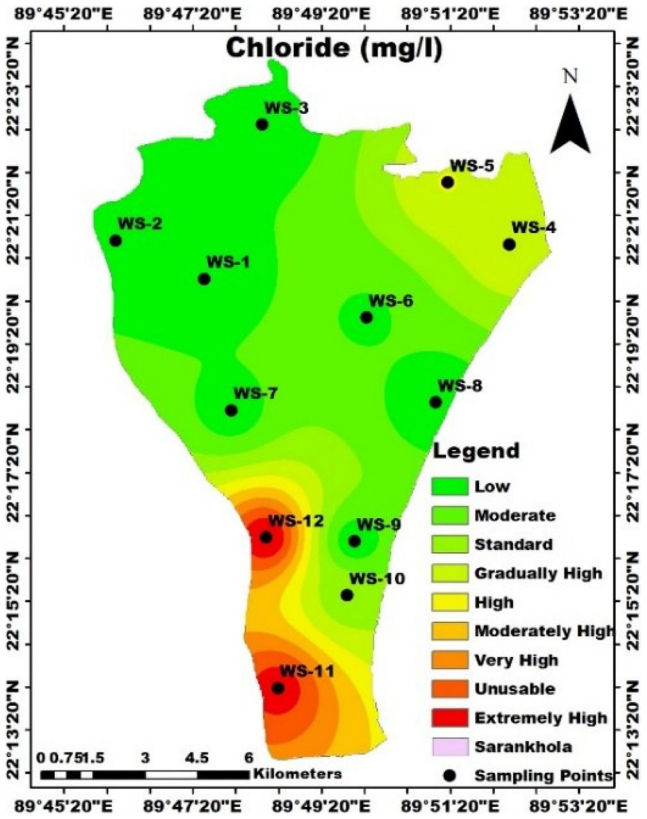

Fig. 9 Spatial map for Cl- (mg/l) availability of water in study area

Cl^-, with WS-12 recording 4250 mg/l. The average value of the Cl^- concentration of Sarankhola Upazila is 1212.83 mg/l, which is around six times greater than the standard value. WS-12 Cl^- concentration (4,250 mg/l) was 7 times higher than the WHO limit (600 mg/l). The reason behind this high Cl^- concentration might be saltwater, as there is no industrial activity found in that area that causes this salinity. Cl^- are abundant in seawater, usually present at concentrations of 19,000 mg/l, which is significantly higher than that of freshwater. According to a study, groundwater salinity is still high eight years after a storm surge, especially in low-lying locations, which impacts both surface and drinking water sources (Tsai et al. 2024). The increased Cl^- levels are likely caused by tidal effects and seawater intrusion rather than industrial effluents because there are no industrial sources present.

Na^+ concentration

Both fresh and saltwater frequently include Na^+ ions, which are very soluble. In saline water sources, they are among the primary cations. With maximum concentrations of 5040 mg/l and 4700 mg/l in Southkhali union, WS-4, WS-5, WS-6, WS-7, WS-10, WS-11, and WS-12 surpass standard limits (Fig. 10). Na^+ levels in WS-12 (5,040 mg/l) exceeded the standard by 10 times. The average value found is also significantly higher than the standard value. This indicates that salinity has an impact on water sources. Elevated salt levels harm crops, deteriorate soil quality, and are harmful to health, especially for those who have high blood pressure. According to a study, cyclone impacts caused a significant shift in salinity profiles, with pre-monsoon salt levels rising from 21.2 ppt in 2017 to 32.6 ppt in 2021. Cyclones like Fani, Bulbul, Amphan, and Yaas were blamed for the seawater intrusion that led to the rising salinity trend (Chowdhury et al. 2023).

Soil salinization

It is essential to analyze some of the soil parameters, including EC, N, P, K, and pH, to evaluate soil quality and nutrient availability, measure the salinity extent and status, and identify the potential impacts of salinity on agriculture (Khanam et al. 2020). Low atmospheric pressure causes storm surges that allow saltwater intrusion, which degrades soil quality. The soil samples were tested for the parameters that imply the soil salinity and compared with the standard values to evaluate the extent. The detailed soil quality measurements of Supplementary Table 2 have been summarized here to make them clear. The EC of the soil was between 647 and 8486 µS/cm, and Southkhali had the highest salinity level, which was highly above the standards of SRDI (2000–4000

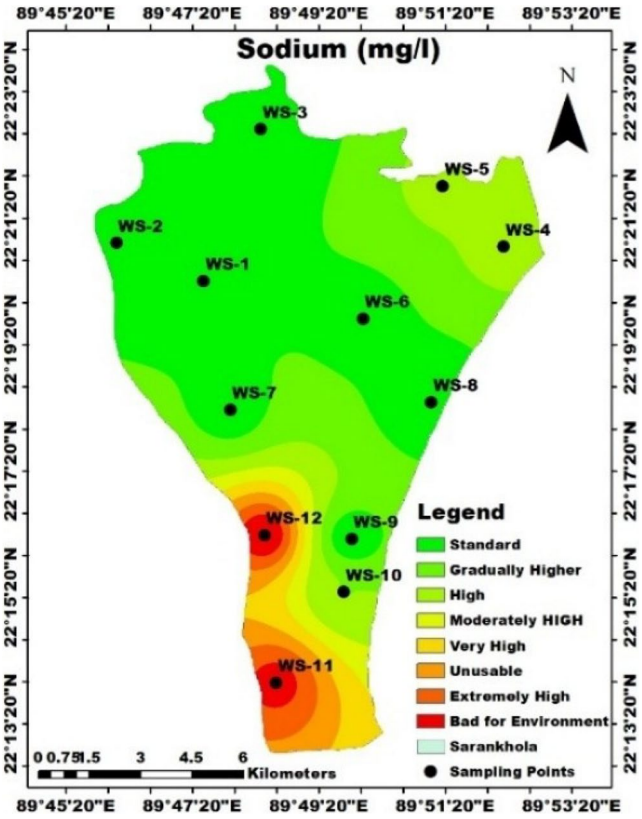

Fig. 10 Spatial map for Na^+ (mg/l) availability of water in study area

µS/cm). The mean soil EC was recorded to be 3480.67 µS/cm as a mean of all the sites, which reflected that there was general salinity stress. The pH of the soil was found to be between 6.11 and 7.10, and the majority of the samples were slightly below the optimum level (6.5 to 7.5). There was a significant discrepancy in nutrient concentrations; N, P, and K were found in the ranges of 48–599 mg/kg, 64–936 mg/kg, and 118–1622 mg/kg, respectively, with the most extreme values occurring in Southkhali. Such results highlight intense salinity encroachment and imbalance of nutrients in regions that are impacted by the cyclone. The full datasets are presented in Supplementary Table 2.

Soil pH

Soil can be categorized into three main classes depending on pH: acidic soil (pH < 6.5), normal soil (pH 6.5–7.8), and alkaline soil (pH > 7.8) (Kadam 2016). While six sampling stations (SS-2, SS-3, SS-6, SS-9, SS-10, and SS-11) were within the ideal range, six others showed acidic conditions. For the majority of agricultural activities, a pH of 6.5 is suitable. According to the spatial map (Fig. 11), the most acidic areas are SS-2, SS-6, and SS-10, which are situated in Dhansagar, Khontakata, and Southkhali Union. The fact that different places have different pH values emphasizes how saltwater intrusion affects soil acidity.

Soil salinity (EC)

The EC of soil determines how well it conducts electricity. EC is a key indicator of soil nutrient availability and fertility. The EC shouldn't be too high, like most other things in the soil, because too many nutrients, particularly Na^+ and Mg, can harm soil health. Soil EC should therefore be between 110 and 570 mS/m (Kamran et al. 2024), whereas the study area exhibits elevated EC values. In Southkhali Union, SS-10 had the highest EC (8486 µS/cm), while SS-8 had the lowest (647 µS/cm). Southkhali's soil EC (8,486 µS/cm) was 2.4 times higher than SRDI's upper limit (3,500 µS/cm). Although the average EC (3480 µS/cm) indicates a modest salinity throughout the region, there are a few places where the salinity is higher than what is acceptable for plant growth. The most salinized area on the spatial map (Fig. 12) is SS-10, which is associated with tidal waves and storm surges that introduce dissolved salts into the soil. Reduced agricultural productivity and drought stress result from high EC, which interferes with plants' ability to absorb water (Dasgupta et al. 2015).

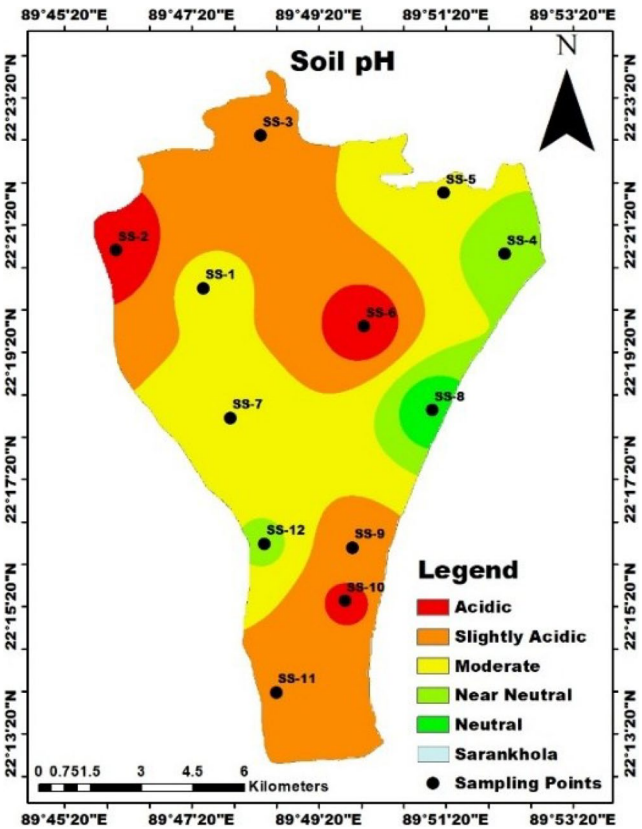

Fig. 11 Map for soil pH availability in study area

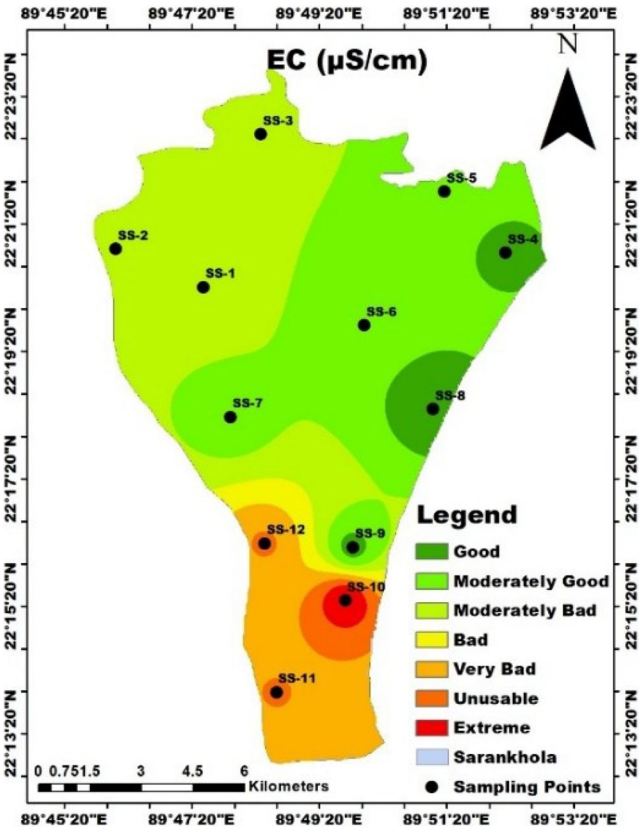

Fig. 12 Spatial map for soil EC (µS/cm) availability in study area

N

From the spatial map (Fig. 13), it is observable that 67% of the sampling points are highly abundant with N, and only one sampling point has N deficiency, which is only 48 mg/kg. The majority of the sampling locations—especially SS-10, SS-11, and SS-12 in Southkhali—show high levels of N, making them unsuitable for agriculture. This excess of N can be related to the breakdown of organic matter, domestic wastewater, and restricted plant uptake because of saltwater. Elevated N levels further hinder plant growth by exacerbating osmotic imbalance and salt stress.

P

The ideal range of P availability is between 150 and 200 mg/kg, with SS-10 having the highest content (936 mg/kg) and SS-8 having the lowest (50 mg/kg). P in SS-10 (936 mg/kg) was 4.6 times higher than the optimum range (150–200 mg/kg). There might be multiple reasons for P abundance, one of which is agricultural runoff and sediment deposition from rivers. Spatial analysis confirms the high P enrichment of SS-10 and SS-11, potentially leading to nutrient imbalances and disrupting microbial activity. Mycorrhizal fungi help accumulate nutrients from the soil, but high salinity can stress these fungi, preventing them from assisting in P accumulation and thereby disrupting P availability for plants (as shown in Fig. 14).

K

The majority of sampling sites have noticeably elevated K levels, with SS-10 having the highest value (1622 mg/kg). A high abundance of K might hamper other nutrient availability. Additionally excess K causes clogged pore space in soil, which retards water infiltration and leads to water logging. Almost 90% of the sampling points have high concentrations of K. Only one sample is in an optimum range, which is SS-8. SS-10 has the most abundance, which is 1622 mg/kg. The lowest among the ranges is 275 mg/kg, which was found in SS-9. K buildup is probably influenced by the intrusion of seawater and the breakdown of mangrove plants. High salinity and excess K exacerbate osmotic stress, reducing plant water intake and interfering with enzyme function. Declining soil health negatively impacts agriculture, as indicated by elevated EC, acidic pH, and high NPK levels. According to a spatial study, the most affected area is the Southkhali Union, especially SS-10. We need adaptive agricultural techniques and sustainable soil management to address these issues (as shown in Fig. 15).

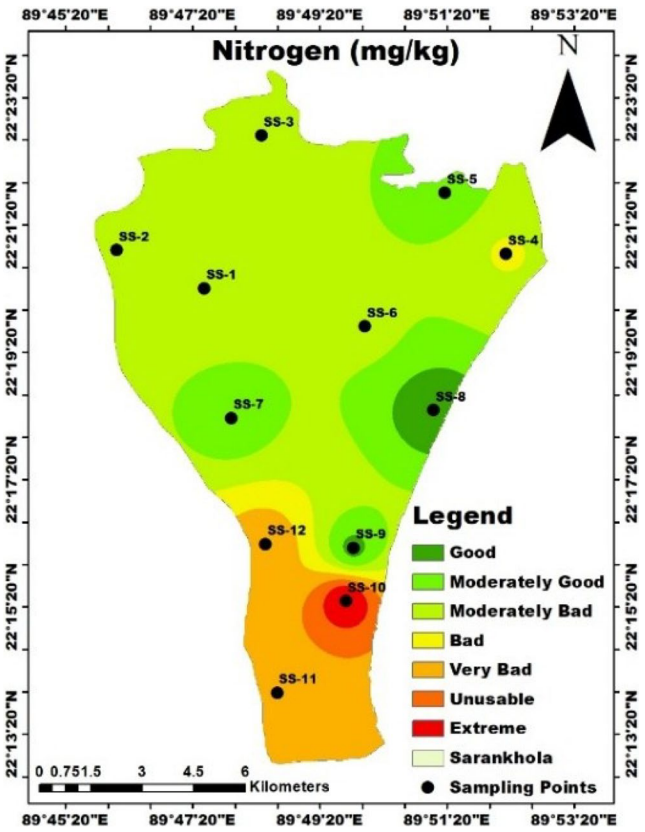

Fig. 13 Spatial map for soil N (mg/kg) availability in study area

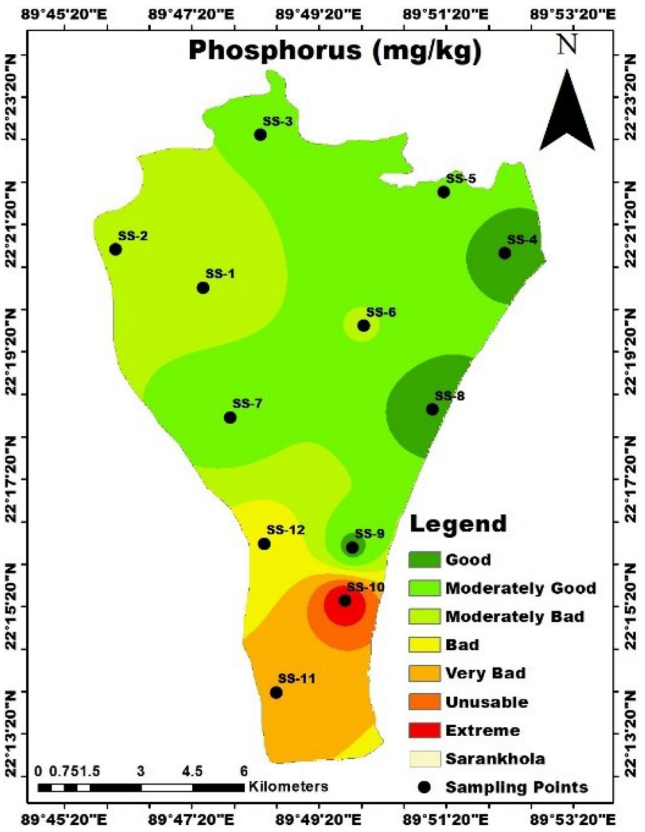

Fig. 14 Spatial map for soil P (mg/kg) availability in study area

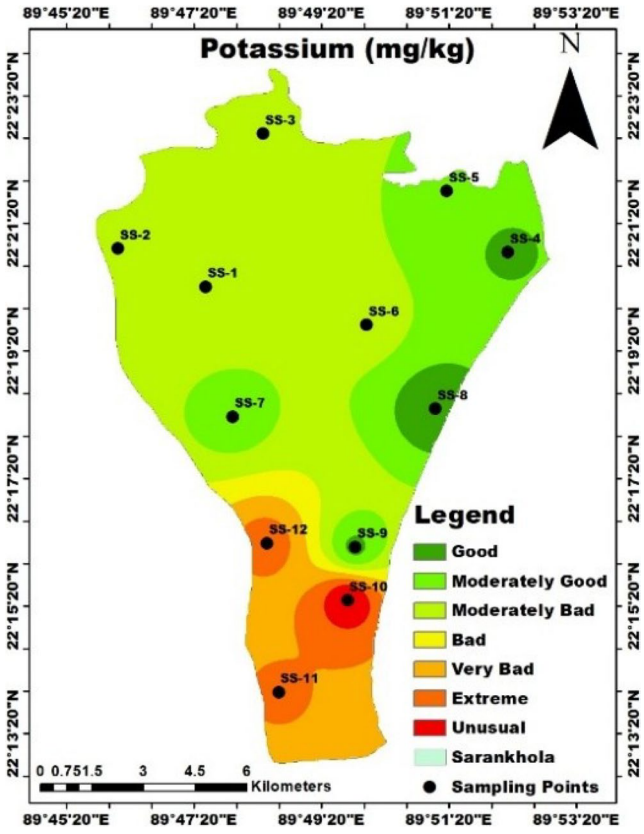

Fig. 15 Spatial map for soil K (mg/kg) availability in study area

Principal component analysis (PCA)

To identify the dominant factors influencing the water and soil quality, PCA was performed on the datasets. The water parameters (pH, EC, TDS, HCO_3^-, Cl^-, and Na^+) explained 94.04% of PC1 (=83.74) and PC2 (=10.3) of the total variance. PC1 had a significant correlation with the salinity-related variables (EC, TDS, Na^+, Cl^-), and PC2 was mostly affected by pH. HCO_3^- showed a strong negative loading on PC3 thus showing a different behavior compared to all the other parameters. The PCA biplot (Fig. 16a) shows that the samples of Southkhali are clustering around the high salinity variables, which proves the high level of seawater intrusion. (Table 7.)

In soil parameters (Temperature, EC, pH, N, P, K), the first two components, PC1 (=70.79) and PC2 (=15.55), accounted for 86.34% of the variance. PC1 was mostly made up of EC, N, P, and K, which means that salinity and nutrient enrichment were the main causes. Temperature and pH, on the other hand, had an effect on PC2. The PCA biplot (Fig. 16b) shows that Southkhali samples group together in areas with high salinity and nutrients, which implies that the soil is out of balance and getting worse because of the cyclone's salinity. (Table 8.)

Satellite data analysis

NDVI

Cyclone 'Remal' made landfall in the southwestern coastal districts of Bangladesh. Appreciatively, the Sundarbans protected thousands of people and their belongings by acting as a barrier. However, the Sundarbans' greenery suffered severe damage in return. The overall NDVI change and increase in water bodies provide insight into the changes. NDVI, a remote sensing method that uses visible and near-infrared (NIR) reflectance to

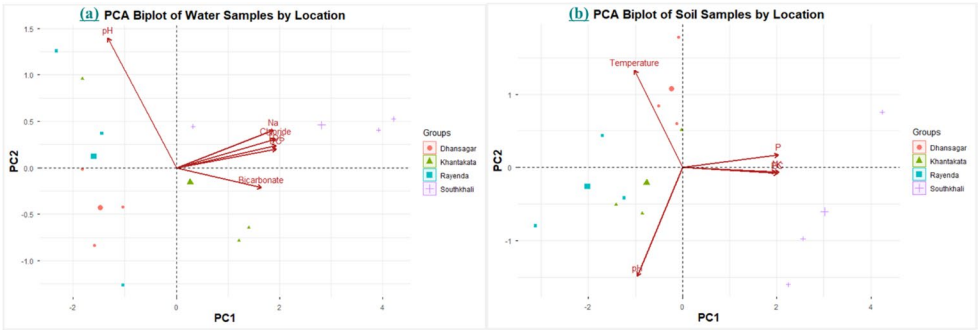

Fig. 16 PCA biplots for water and soil samples by location; (**a**) PCA biplot of water samples, (**b**) PCA biplot of soil samples

Table 7 PCA loadings and variance for water parameters

EC	PC1	PC2	PC3	PC4	PC5	PC6
	0.44	0.13	0.07	−0.55	−0.45	−0.52
TDS	0.44	0.16	0.12	−0.31	−0.07	0.82
pH	−0.3	0.91	−0.28	−0.06	−0.01	0.01
Na^+	0.43	0.26	0.25	0.76	−0.33	−0.06
HCO_3^-	0.38	−0.14	−0.91	0.14	0.01	0.01
Cl^-	0.44	0.2	0.15	−0.03	0.83	−0.24
Variance (%)	83.74	10.3	5.68	0.27	0.01	0

Table 8 PCA loadings and variance for soil parameters

Temperature	PC1	PC2	PC3	PC4	PC5	PC6
	−0.24	0.66	−0.7	−0.02	0.07	−0.05
EC	0.47	−0.04	−0.21	−0.36	0.31	0.71
pH	−0.22	−0.74	−0.62	−0.04	−0.07	−0.06
N	0.46	−0.03	−0.2	0.86	0.09	0.03
P	0.47	0.08	−0.15	−0.2	−0.83	−0.1
K	0.48	−0.03	−0.09	−0.3	0.44	−0.69
Variance (%)	70.79	15.55	11.75	1.41	0.4	0.1

estimate vegetation health, showed significant variations. In contrast to lower values, which denote sparse vegetation or barren land, high NDVI levels represent dense, healthy vegetation.

The classified image before and after the cyclone indicates slight changes. In Fig. 17, it is visible that the water bodies have increased slightly while decreasing the vegetation area. As most of the vegetation is situated in the Sharankhola range of Sundarbans, it can be said that Cyclone Remal's wind gusts gravely damaged the study area's vegetation state. The NDVI algorithm successfully distinguished between dense and sparse vegetation and between vegetation and non-vegetation. To categorize barren terrain, settlement, infrastructure, and water separated from the land, the primary criteria were object brightness, area, length, length/width ratio, and mean of red and NIR bands (Islam et al. 2023). In this study, a very helpful tool for classification was the mean of red and NIR bands. According to the findings (Fig. 18), sparse vegetation decreased from 201 square kilometers to 159 square kilometers (decreased by 22%), resulting in a loss of 104 square kilometers of vegetation. The cyclone's effects particularly impacted deep vegetation areas, causing the most damage.

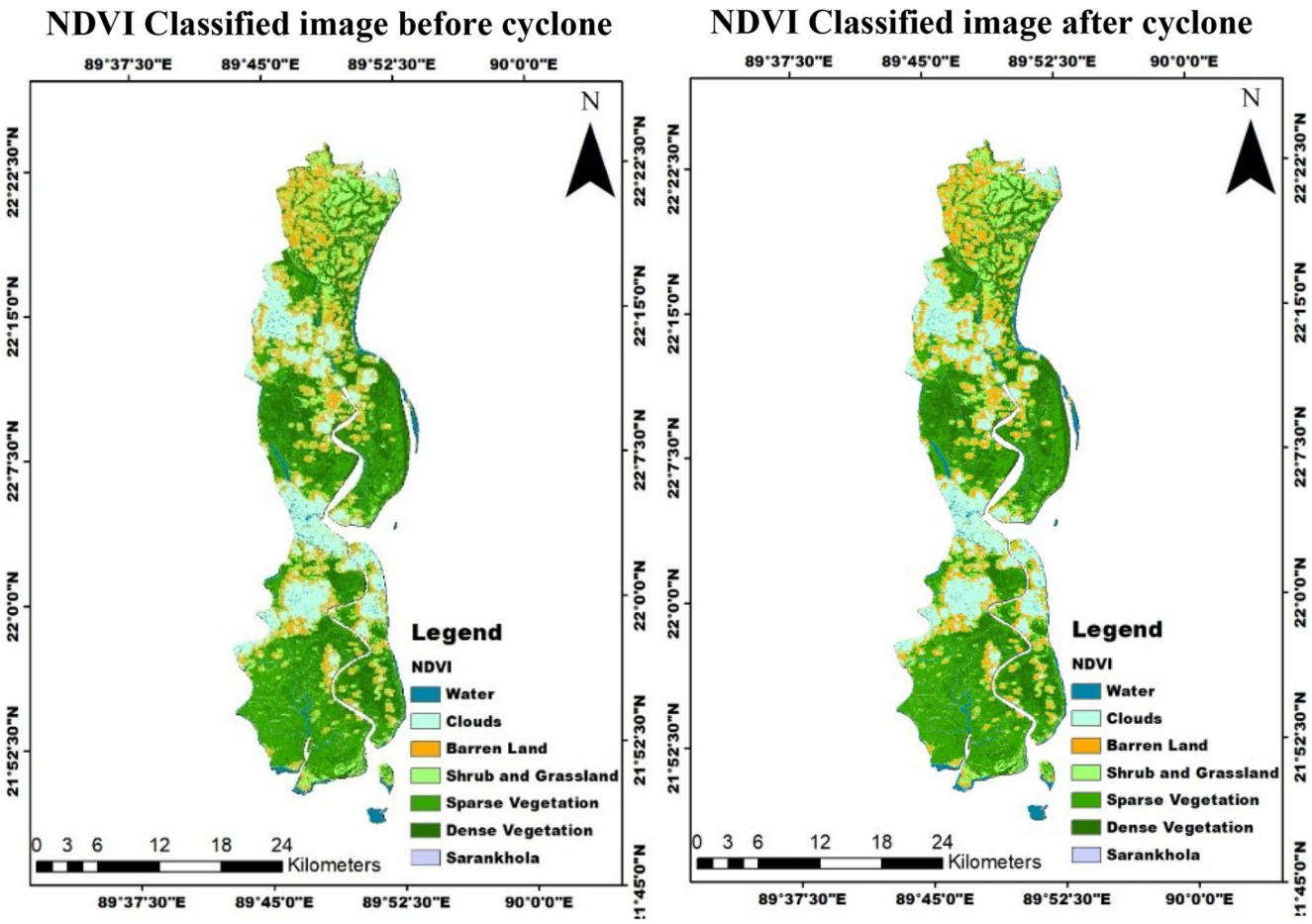

Fig. 17 Study site Sarankhola Upazila showing pre- and post-cyclone images acquired on 16 May 2024 and 07 June 2024, respectively, with the used NDVI classification schemes

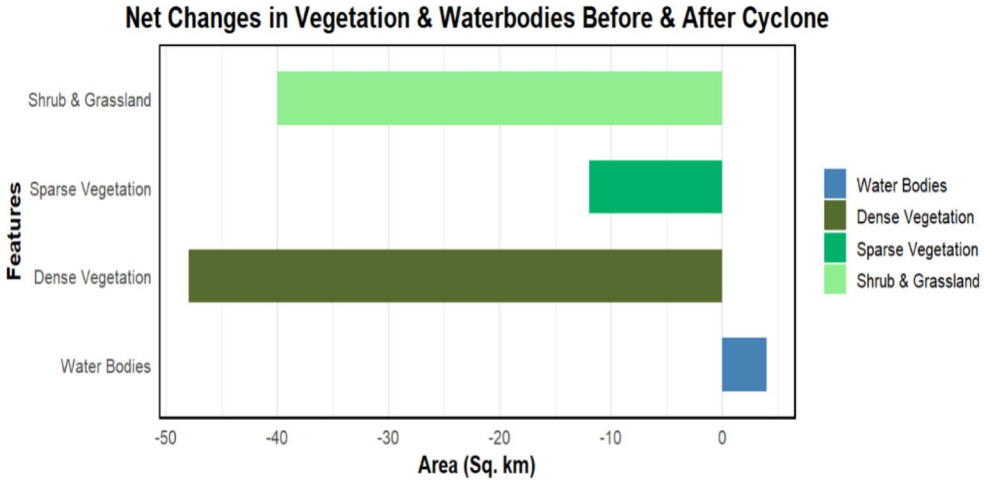

Fig. 18 Net Changes of vegetation in Sharankhola due to Cyclone 'Remal'

The cyclone's increased water covering and decreased vegetation also resulted in the loss of wildlife habitat. The arid area was submerged by heavy rainfall and high tides, and water features, such as rivers and canals, grew from 21 to 24 square kilometers (increased by 14%).

At the same time, grassland and shrubs decreased from 90 to 78 square kilometers, while bare ground grew from 97 to 103 square kilometers. Figures 17 and 18 represent the results of vegetation change identification that was performed before and after Cyclone 'Remal,' which is why significantly deforested lands and the corresponding increase of water masses are evidenced.

NDSI

Even though traditional techniques like laboratory tests and field surveys can produce precise mapping of soil salinity, they are labor-intensive, expensive, and time-consuming, particularly for large-scale surveys. A possible method for determining soil salinity and, eventually, creating EC maps is multispectral instrument (MSI) images (Xu et al. 2020; Gerardo and De Lima 2022). The most sensitive bands to the ions in the soil that induce salinity are the Red and NIR bands, which are used to determine NDSI (Konukcu et al. 2006; Nguyen et al. 2020).

An effective substitute for mapping soil salinity is NDSI, which is obtained from Sentinel-2 images and uses the red and NIR bands to identify areas that are impacted by salt as shown, in Fig. 19. Pre- and post-cyclone comparisons reveal a move toward higher salt levels, with high NDSI values signifying increased salinity.

High-salinity regions increased from 10 to 15 square kilometers (expanded by 50%) after Cyclone 'Remal,' whereas non-saline areas decreased from 59 to 25 square kilometers (shrank by 58%) (Fig. 20). Significant saltwater intrusion brought on by the storm surge is indicated by the growth of high-salinity areas and the decrease of low-salinity zones. The cyclone's effect on soil degradation is highlighted by the rise in moderate and high saline levels that followed. Figures 19 and 20 illustrate salinity before and after Cyclone 'Remal' by using the NDSI to summarize net changes. The resulting maps show an extension of the high-salinity areas alongside a contraction of non-saline ones in the post-Cyclone 'Remal' period.

Soil salinity index (SI_ASTER)

Soil salinity levels can be efficiently distinguished using the Soil Salinity Index (SI_ASTER), which is based on shortwave infrared (SWIR) bands. The Salinity Index ASTER has been used in many investigations with data from Sentinel-2, Landsat-ETM+, and Aster satellites. It can be applied to differentiate between various soil salinity levels (Sun et al. 2021). ASTER_SI values that are close to −1 signify low salinity of the soil (Azabdaftari and Sunar 2016; Shukurov 2020).

Five classifications of salinity were established by Sentinel-2-based analysis: non-saline, slightly saline, moderately saline, highly saline, and very highly saline. An overall observation of the salinity index shows that the region's salinity has increased due to the cyclone; places that were previously less affected after the cyclone have moderate to extremely high salinity.

High-salinity areas significantly increased after the cyclone, while non-saline land decreased from 13 to 10 square kilometers (decreased by 23.1%), and very high salinity areas increased from 74 to 87 square kilometers (expanding by 17.6%) (Fig. 22). Low-salinity areas were transformed into highly salinized areas by the storm surge brought on by the cyclone, which allowed saltwater intrusion. These graphics enable additional research on the cyclone's effects on agriculture and freshwater availability by illustrating how it affected the salinity of the soil and water. Figures 21 and 22 show salinity maps based on the SI_ASTER algorithm of the pre- and post-cyclone periods, which in turn highlights a spatial redistribution of the high classes of salinity.

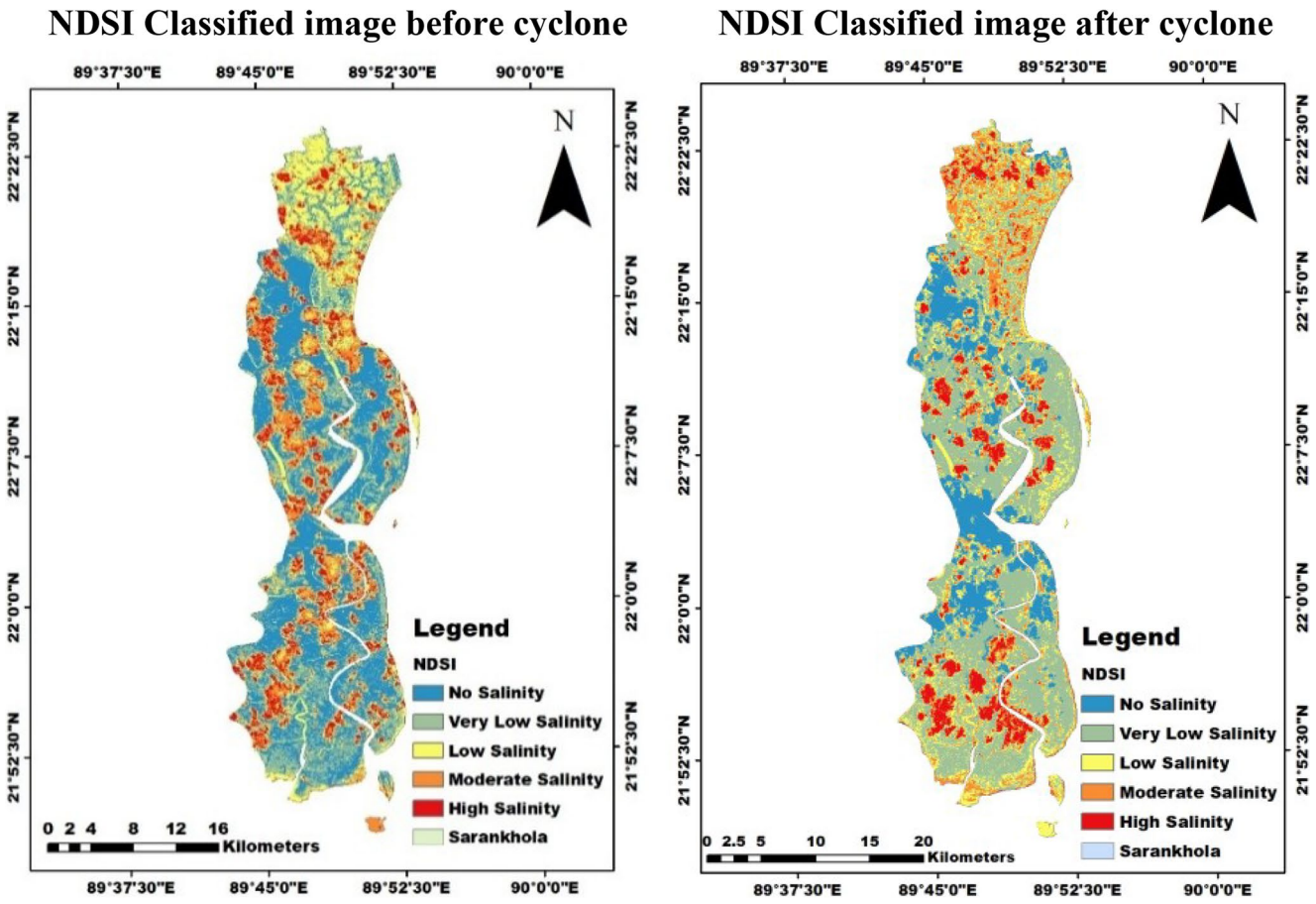

Fig. 19 Study site Sarankhola Upazila showing pre- and post-cyclone images acquired on 16 May 2024 and 07 June 2024, respectively, with the used NDSI classification schemes

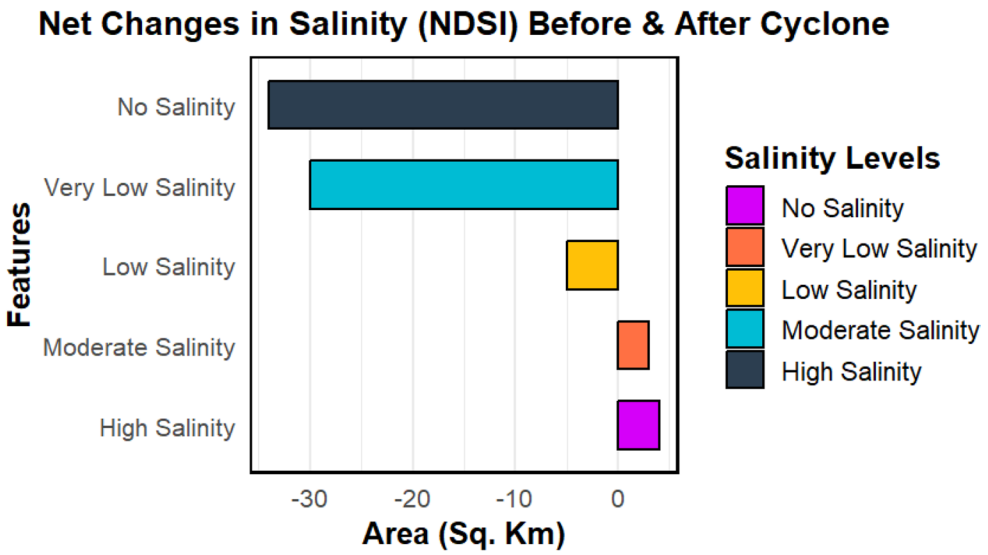

Fig. 20 Net changes of salinity in Sharankhola due to Cyclone 'Remal'

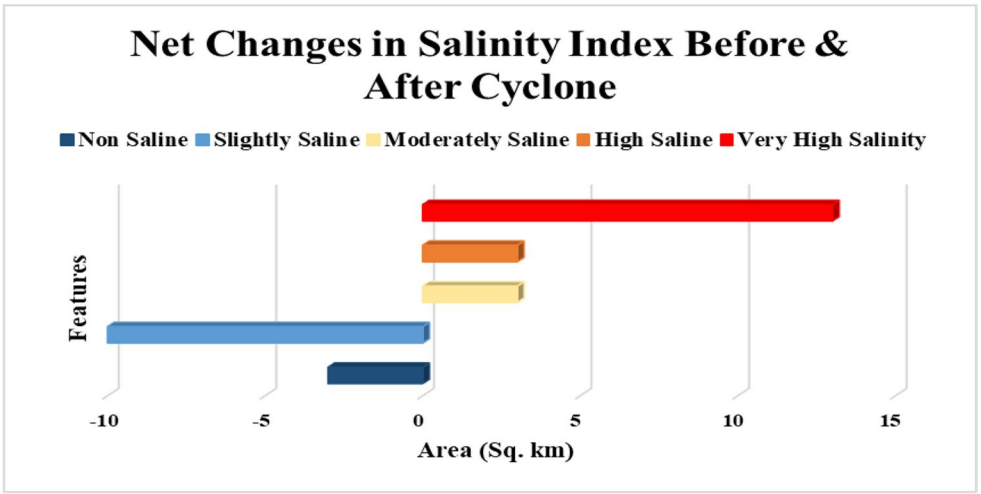

Fig. 22 Net changes of Salinity Index (ASTER) in Sharankhola due to Cyclone 'Remal'

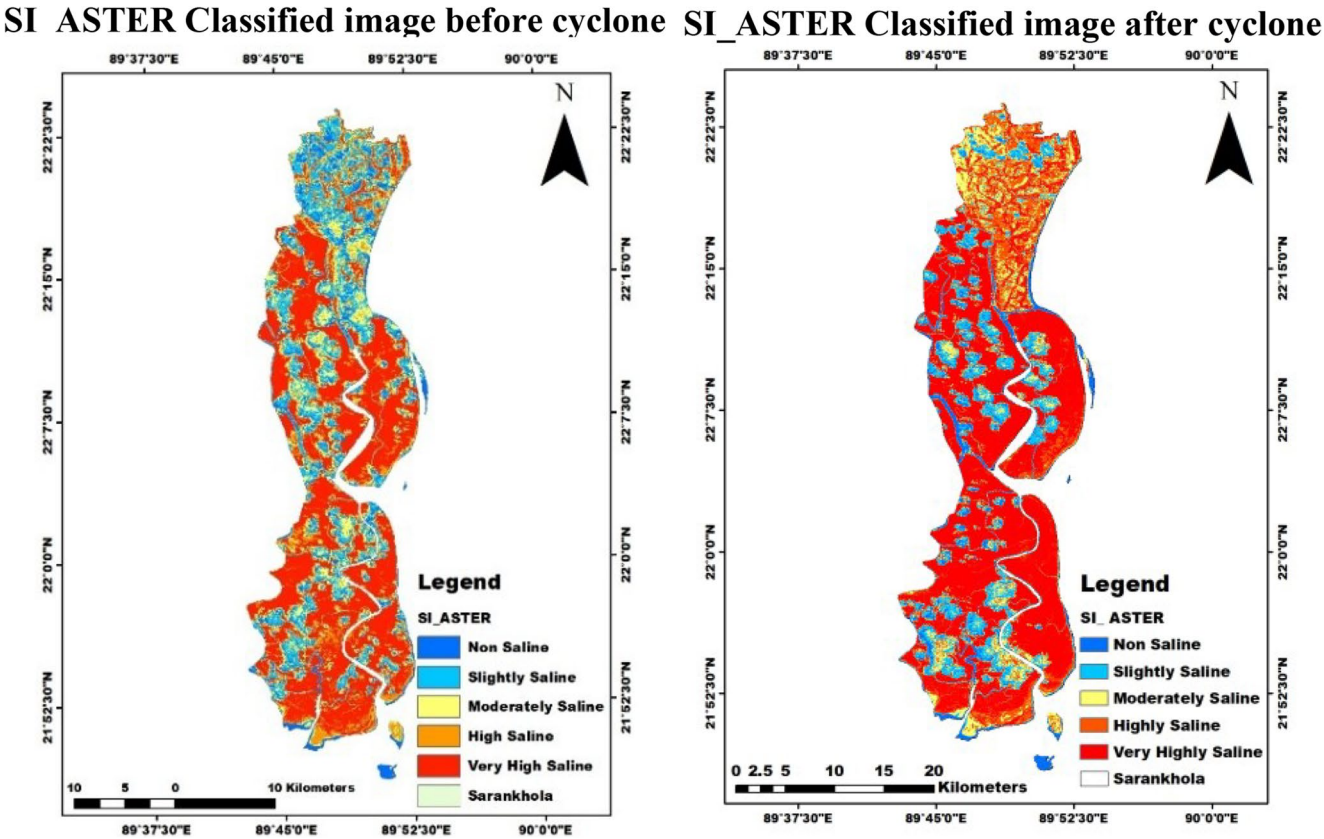

Fig. 21 Study site Sarankhola Upazila showing pre- and post-cyclone images acquired on 16 May 2024 and 07 June 2024, respectively, with the used SI_ASTER classification schemes

Discussion

This study tries to demonstrate Cyclone 'Remal' induced salinization across waterbodies and soils in a coastal region of Bagerhat (Sarankhola) with the highest EC/TDS and major ions (Na^+, Cl^-) concentrated in Southkhali. The combination of point-based chemical measurements (pH, EC, TDS, HCO_3^-, Na^+, Cl^-, NPK), multivariate statistical analysis (PCA), and the indexes generated by Sentinel-2 (NDVI, NDSI, SI_ASTER) generated complementary evidence where field measurements were used to define the extent and compositional range of salinity and nutrients, and satellite indices were used to estimate the spatial distribution and temporal change after the event. These mixed methods study

explicitly address the limitations that were observed in previous studies that did not employ integrated spatial analysis and systematic evaluation of the effects of mitigation (Haq et al. 2024). The rationale of using salinity indices such as the SWIR-based SI_ASTER and red-NIR/SWIR combinations to map the salinity of the soil in agriculture contexts and deltaic areas is based on previous evidence of the sensitivity of SWIR bands to salt minerals and the usefulness of these indices to map soil salinity (Gerardo and De Lima 2022; Geopera 2024). The patterns of salinity post-cyclone that we observed (sharp peaks of EC/TDS, an increase in high-salinity areas by approximately 17.6%, and a decrease in non-salty areas by approximately 23.1%) are in line with the multi-decadal patterns of salinity in the coastal delta of Bangladesh. The freshwater-brackish boundary in the moribund delta north of the Sundarbans shifts northwards (along the dry season) by about 20–40 km, and cataclysmic surges of salinity are associated with inconsistency in upstream discharge and intermittence in cyclones; recovery is enhanced in reaches with greater flushing of rivers (Haq et al. 2024). Numerical and field studies suggest that storm-surge overtopping, or breaches, can readily salinize ponds and shallow groundwater, with sediment salt 'memory' potentially maintaining elevated salinity for months to years unless prompt remediation occurs (Tsai et al. 2024). Outside Bangladesh, post-cyclone Amphan occurred in 2020 and Bulbul occurred in 2019 results were reports of NDVI/EVI degradation and NDSI increase and barren land growth, trends that our NDVI drop and salinity index growth followed (Jaman et al. 2019; Prakash et al. 2023). Stress of mangroves and canopy increase related to shoreline change and salinity increase in the Sundarbans is also observed by multi-year geospatial analysis and supports the generality of our findings (Islam et al. 2015). The extreme post-cyclone shifts in soil N and P (especially in Southkhali) are probably due to the interaction of hydrological and biogeochemical processes; storm-surge seawater intrusion and waterlogging decrease plant uptake and oxygen in the root zone and change the decomposition to anaerobic pathways that break down organic N and P more quickly than plants can, thereby accumulating nutrients in soils (Sultan et al. 2023). Agricultural residues and fertilizers deposited during floods become trapped in depressions and low-permeability layers; diminished drainage and reduced leaching transpire in saline conditions, which further promote local enrichment (Feist et al. 2023; Shapna et al. 2024). Active transport in roots is inhibited at high EC by ionic competition and osmotic stress to create nutrient imbalances (e.g., high K interferes with Ca/Mg uptake) and instead leads to the accumulation of available N and P in soil solution instead of biomass (Sultan et al. 2023). All concur with case studies on Bangladesh that link cyclones to transient salinity elevations (most evident with early monsoon landfalls) and alterations in nutrients through the inundation mechanism (Haq et al. 2024; Rahman et al. 2025). High EC (up to approximately 10000 µS/cm), Cl^- (>4000 mg/l), and Na^+ (>4700–5000 mg/l) make irrigation water inappropriate and lead to osmotic stress and yield reduction, especially in the coastal belt (rice and vegetables). Quantitative estimates indicate that climate-driven salinity changes could reduce regional income due to increased salinity levels in coastal Bangladesh, particularly affecting high-yield rice crops. Regional income losses are estimated to decrease by 15.6% in subdistricts with a soil EC of >4 dSm^{-1} (soil EC) when adaptation measures are implemented (Dasgupta et al. 2014, 2015). In the case of freshwater fisheries, the surges leading to high EC and Cl^- increase levels negatively affect the spawning, larval survival, and pond ecology (field observations and models of ponds and shallow aquifers are always salinized). Policy syntheses indicate that rainwater harvesting, sluice/embankment management, and freshwater injection (e.g., Managed Aquifer Recharge) are viable solutions for securing aquaculture and agriculture, which our spatial maps can support (Scheltinga et al. 2024; Shapna et al. 2024).

The salinity sustainability history is dual-phase. Storm-surge events result in swift elevations (in EC/TDS) and a decline in vegetation health (reduction in NDVI) in the short term (weeks to months) (Jaman et al. 2019; Prakash et al. 2023). Long-term persistence (over seasons to years) depends on the storage of sediment salt and the evapoconcentration that occurs during the dry season, as well as flushing and recurrent storm surges. The empirical time series data from coastal Bangladesh indicates seasonal fluctuations of the fresh-brackish boundary, abrupt salinity occurrences associated with river flow, and a slower recovery in stagnant delta regions (Haq et al. 2024). Hydro Geosphere calculations and on-site observations indicate that, one year afterwards, salinity levels may remain elevated both at the surface and within the shallow groundwater unless early measures are taken to maintain pond remediation and embankment stability (Tsai et al. 2024). PCA revealed consistent factor structures; in water, PC1 integrated EC, TDS, Na^+, Cl^-, and the salinity-nutrient enrichment axis, whereas PC2 differentiated pH and temperature. In soil, PC1 integrated EC, K, N, and P, representing a salinity-nutrient enrichment axis; PC2 differentiated pH and temperature. These elements describe the co-variation between variables and explain why Southkhali is associated with all high salinity and NPK. Multivariate factorization has been extensively used to differentiate environmental factors in waterbodies and soils, and our PCA serves as a complement to geospatial indices through dimensionality reduction and latent gradient identification, elucidating the foundation of the spatial salinity mosaic (Ahamad et al. 2020; Li et al. 2021). Our remote

sensing selections (NDVI, NDSI, SI_ASTER) exemplify recognized salt/vegetation sensitivity in agricultural and delta studies (Gerardo and De Lima 2022). The conceptual links between ecological risk and source apportionment frameworks in hypothetical and sediment research (identifying contaminated sources and hazards through multivariate methods) demonstrate conceptual similarities (Ahamad et al. 2020; Li et al. 2021). Experiments on the River Ravi in Pakistan reveal that physicochemical stresses associated with water quality, such as metals, adversely affect aquatic life and may result in systemic concerns, serving as a cautionary comparison for the salinity-induced fishing issues encountered in coastal Bangladesh (Akhtar and Nawaz 2012; Ahamad et al. 2024a). Geotechnical site characterization of soft, saline sediments (e.g., Lake Urmia) is employed to comprehend the influence of soil properties (compressibility, stratigraphy, permeability) on water-solute transport, embankment performance, and salt retention, which is pertinent to polder integrity and drainage projects in coastal Bangladesh. Such site investigation protocols (CPTu, ANN-assisted property estimation, optimal investigation design) would help enhance the hydro-geotechnical model of surge infiltration and recovery planning of salinity-prone grounds (Yang et al. 2019; Akbarimehr et al. 2020; Eslami et al. 2020). According to this finding, several directions can be suggested in the future. Hydrological–hydrogeological modeling of surge inundation, salt transport, and sediment memory, including scenario testing (rapid pond clean-up, embankment overtopping, controlled aquifer recharge); recent simulations and field campaigns in Bangladesh (San Tsai et al. 2020, 2024). Monitoring over long periods, incorporating two fortnightly EC/salinity fixed stations during dry and monsoon seasons, and contrasting them will facilitate the seasonal contour migration and recovery difference between the active and moribund delta reaches (Haq et al. 2024). Socio-economic impact analyses, such as yield/income loss estimation during salinity stress of large crops and fishery productivity effects, combine with the adaptation portfolio (sluice/embankment management, rainwater harvesting, MAR, and salt-tolerant varieties) found in practitioner reviews (Scheltinga et al. 2024; Shapna et al. 2024). Cross-hazard risk frameworks, which borrow ecological risk/source-identification literature to co-assess salinity and co-stressors (e.g., contaminants), which in combination influence coastal livelihoods (Li et al. 2021; Ahamad et al. 2024b). New studies also demonstrate the suitability of geospatial methods in environmental stressors and risk assessment, microbial remediation measures against soil pollutants, and multifaceted frameworks for assessing the ecological and human health hazards of toxicants (Ahamad et al. 2024b; Ashraf et al. 2024; Gul et al. 2024), which can be combined with the salinity-focused adaptation planning in coastal systems. To parameterize permeability/compressibility and embankment integrity in hydro-geotechnical models to enhance the design of drainage upgrades in saline and soft sediments, site-specific geotechnical investigations (CPTu, lab tests, and property estimation by data) are used to engineer drainage and levee upgrades (Eslami et al. 2020; Akbarimehr et al. 2024). The evidence of this study includes field chemistry, PCA axes of salinity-nutrient co-variation, and satellite-based salinity/vegetation maps, which all favor location-specific adaptation. Expeditious post-surge pond remediation, drainage restoration, and embankment reinforcement are the primary measures in Southkhali that can guarantee the long-term prevention of salinization (Feist et al. 2023; San Tsai et al. 2024). Rainwater harvesting, salt-resistant crop cycles, and select freshwater discharges should stabilize production in Khontakata and nearby regions of moderate salinity (Scheltinga et al. 2024; Shapna et al. 2024). Since we found a forceful connection between the NDVI decrease and the NDSI increase in our maps and in cyclone case studies, the ecosystem-based interventions (mangrove restoration, green buffers) should be considered to safeguard soils, alleviate the surge power, and accelerate the ecological recovery process (Prakash et al. 2023; Islam et al. 2023).

Limitations

The study sample was small (12 soil and 12 water samples), which was intended to respond to spatial variations across the unions and near-shore-inland differences in an affected region. Although this method sufficed in identifying patterns, it restricts the extrapolation of patterns on a site level, which should be understood as an indication and not a reflection of the large population. Besides, budgetary limits restricted the coverage of the sampling density and the possibility of repeated seasonal field campaigns. Nevertheless, we partially overcame a limitation posed by a small sample size by using a systematic sampling design to cover important spatial variability. The research effort constituted a singular post-event study; recurrent seasonal sampling would more effectively characterize recovery trajectories and dry season evapoconcentration (Haq et al. 2024). Development of remote sensing applications will be advanced in the future by calibration of satellite-derived dry seasons against locally measured ground truth (e.g., EC in dS m^{-1}) to enhance the precision of operation. Even though this calibration was supposed to be done, pre-cyclone ground truth data were not available in this study area, so this limited its application in the current work. Despite these shortcomings, the research provides useful information on the processes of post-cyclone salinity and

proves the effectiveness of using the combination of field measurement and satellite-based methods to assess the environment in a short period of time.

Conclusion

After analyzing the primary data, this study concludes that Cyclone Remal-induced storm surges have caused an important change in the salinization of soil and water in the coastal region of Bagerhat (Sarankhola). Most of the water and soil samples found salinity levels above permissible limits for both human consumption and agricultural use. In particular, the findings revealed strong and spatially uneven salinization with water EC of up to 10,021 µS/cm and soil EC of up to 8,486 µS/cm in the most salinized union (Southkhali), and Na^+ and Cl^- levels that were many times higher than the safe levels. The salinity extremes were associated with a notable nutrient imbalance, particularly elevated levels of N and P, and a statistically significant decline in vegetative health, evidenced by post-cyclone reductions in NDVI and increases in high-salinity groups in NDSI and SI_ASTER diagrams. These results show that salinization, as one of the environmental impacts of a storm surge, is not only a transient environmental issue but also a long-lasting threat to the freshwater sources, the soil's fertility, and livelihood sustainability in the southwestern region of the Bangladesh coast. This study further assumes that storm surges of considerable magnitude will occur often, worsening the already dire situation of soil and water salinization in the southwestern coastal areas of Bangladesh. These extreme weather events are occurring more frequently due to climate change, endangering both the availability of drinking water and viable agriculture. Long-term exposure to excessive alkalinity and salinity levels might lower crop yields, worsen soil biogeochemical processes, and threaten residents' access to fresh water. Climate change is predicted to worsen salinization, bringing more frequent and powerful cyclones. Both short-term and long-term adaptation strategies are required to mitigate these effects. The result highlights the necessity of integrating salinity risk considerations into coastal land-use planning, embankment design standards, and climate-resilient water resource management systems. The study highlights the necessity of integrating salinity risk considerations into coastal land-use planning, embankment design standards, and climate-resilient water resource management systems. These results underscore the crucial need to integrate the salinity risks induced by storms into coastal planning and disaster management strategies. The fact that after storm surge events, it is still observed that high soil and water salinity levels remain is a sign that there is the immediate need to enhance the integrity of embankments and the operation and maintenance of sluice gate systems, as well as adaptive tidal river management to minimize frequent saltwater intrusion. Other disaster preparedness plans should involve the cleanup of the ponds right after the cyclone, covered freshwater, and timely damage assessments to sustain drinking water and food security. The introduction of quick post-event environmental analysis, such as satellite-based monitoring of salinity and vegetation, would facilitate the authority's giving precedence to the emergency response in the worst-hit areas. Promotion of salt-tolerant crop varieties, an adaptive cropping calendar, and rainwater harvesting can cushion productivity at the agricultural level. The inclusion of these measures in national and local policies for adaptation to climate change will be important in supporting livelihoods in coastal areas in the event of rising frequencies and intensities of cyclones that ought to be reinforced by using agricultural extension facilities and inclusion in national climate adaptation and food security policies. By using structural interventions, including tidal river management, sluice gate systems, and enhanced embankments, saltwater intrusion can be controlled. Non-structural strategies, such as altering land-use patterns and introducing salt-tolerant crops, can also enhance resilience in affected areas. To develop a comprehensive management framework, more thorough research of cyclone events is required that includes predictive modeling of future storm surge periods and their consequences. In the coastal regions of Bangladesh, the ongoing salinization of soil and water resources seriously threatens local livelihoods, food security, and freshwater availability in the absence of dedicated measures. The combined efforts of communities, researchers, and government institutions, along with evidence-based planning, long-term monitoring, and active investment in structural and non-structural adaptation strategies, will be necessary to address the issue of saltwater intrusion and introduce resilience to the coastal areas of Bangladesh in the long term.

Supplementary Information The online version contains supplementary material available at https://doi.org/10.1007/s12517-026-12518-z.

Acknowledgements The authors express their gratitude to the laboratory personnel of the Department of Environmental Science and Engineering at Jatiya Kabi Kazi Nazrul Islam University and the Department of Public Health & Engineering, Central Laboratory, Mahakhali, for their kind support with sample analysis. During fieldwork and data collecting, we also appreciate the great collaboration that was obtained. This study was completed thanks to the encouragement and assistance of peers, faculty, and all other contributors who were not recognized as co-authors.

Author contributions Taposhi Habiba: Conceptualization, Framework, Methodology, Formal Analysis, Data Collection, Data Curation, Software, Visualization, Writing -Original Draft, Writing-Review & Editing, Manuscript Preparation, Investigation. Md. Alim Miah: Su-

pervision, Conceptualization, Project Administration, Methodology, Formal Analysis, Laboratory Analysis, Data Collection, Data Curation, Software, Visualization, Writing-Original Draft, Writing-Review & Editing, Manuscript Preparation. Tajim Ahammad: Methodology, Formal Analysis, Resources, Software, Visualization, Data Collection, Writing-Original Draft, Writing-Review & Editing, Manuscript Preparation. Md Khairul Haque: Formal Analysis, Data Curation, Methodology, Software, Visualization, Writing-Original Draft, Writing-Review & Editing, Manuscript Preparation, Validation.

Funding External funding in any form was not received to support this research study.

Data availability All data supporting the findings of this study are available within the paper and its Supplementary Information.

Declarations

Conflict of interest The authors declare that the research was conducted in the absence of any commercial or financial relationships that could be construed as a potential conflict of interest.

References

Bangladesh Meteorological Department (2024) Bangladesh Meteorological Department. https://live6.bmd.gov.bd/. Accessed 22 June 2024

IFRC (2024) Bangladesh: Cyclone Remal | IFRC. https://www.ifrc.org/emergency/bangladesh-cyclone-remal. Accessed 22 June 2024

The Indian Express (2024) Cyclone Remal to hit Bengal: How and why are cyclones named? | Explained News - The Indian Express. https://indianexpress.com/article/explained/explained-sci-tech/cyclone-remal-bengal-naming-9351508/. Accessed 15 Aug 2024

Ahamad MI, Song J, Sun H et al (2020) Contamination level, ecological risk, and source identification of heavy metals in the hyporheic zone of the Weihe River, China. Int J Environ Res Public Health 17:1070. https://doi.org/10.3390/ijerph17031070

Ahamad MI, Rehman A, Mehmood MS et al (2024a) Spatial distribution, ecological and human health risks of potentially toxic elements (PTEs) in River Ravi, Pakistan: a comprehensive study. Environ Res 263:120205. https://doi.org/10.1016/j.envres.2024.120205

Ahamad MI, Yao Z, Ren L et al (2024b) Impact of heavy metals on aquatic life and human health: a case study of River Ravi Pakistan. Front Mar Sci 11:1374835. https://doi.org/10.3389/fmars.2024.1374835

Akbarimehr D, Eslami A, Aflaki E, Imam R (2020) Using empirical correlations and artificial neural network to estimate compressibility of low plasticity clays. Arab J Geosci 13:1225. https://doi.org/10.1007/s12517-020-06228-3

Akbarimehr D, Rahai M, Ahmadpour M et al (2024) Geotechnical properties of Urmia Saltwater Lake bed sediments. Geotechnics 5:1. https://doi.org/10.3390/geotechnics5010001

Akhtar S, Nawaz M (2012) Impact of Water Quality on Aquatic Life in River Ravi, Pakistan. Nat Environ Pollut Technol 11:219–224

Akhter S, Qiao F, Chowdhury KMA et al (2024) Simulation of the upper oceanic response to the super cyclonic storm Amphan in the Northern Bay of Bengal. J Sea Res 198:102484. https://doi.org/10.1016/j.seares.2024.102484

Akter T, Hoque MA-A, Mukul SA, Pradhan B (2025) Coastal Flood Induced Salinity Intrusion Risk Assessment Using a Spatial Multicriteria Approach in the South-Western Bangladesh. Earth Syst Environ 9:31–49. https://doi.org/10.1007/s41748-024-00399-9

Alex E, Ramesh K, Hari S (2017) Quantification and understanding the observed changes in land cover patterns in Bangalore. IJCIET 8:597–603

Ashraf T, Aslam J, Mehmood MS et al (2024) Geospatial assessment of built environment on land surface temperature in district Sheikhupura, Punjab Pakistan. Discov Geosci 2:30. https://doi.org/10.1007/s44288-024-00035-z

Ashrafuzzaman M, Artemi C, Santos FD, Schmidt L (2022) Current and future salinity intrusion in the South-Western Coastal Region of Bangladesh. Span J Soil Sci 12:10017. https://doi.org/10.3389/sjss.2022.10017

Azabdaftari A, Sunar F (2016) Soil salinity mappiing using multitemporal LANDSAT data. Int Arch Photogramm Remote Sens Spatial Inf Sci XLI(B7):3–9. https://doi.org/10.5194/isprsarchives-XLI-B7-3-2016

Baten MA, Seal L, Lisa KS (2015) Salinity Intrusion in Interior Coast of Bangladesh: Challenges to Agriculture in South-Central Coastal Zone. AJCC 04:248–262. https://doi.org/10.4236/ajcc.2015.43020

Chowdhury A, Naz A, Sharma SB, Dasgupta R (2023) Changes in salinity, mangrove community ecology, and organic blue carbon stock in response to cyclones at Indian Sundarbans. Life 13:1539. https://doi.org/10.3390/life13071539

Dasgupta S, Huq M, Khan ZH et al (2014) Cyclones in a changing climate: the case of Bangladesh. Clim Dev 6:96–110. https://doi.org/10.1080/17565529.2013.868335

Dasgupta S, Hossain MM, Huq M, Wheeler D (2015) Climate change and soil salinity: The case of coastal Bangladesh. Ambio 44:815–826. https://doi.org/10.1007/s13280-015-0681-5

Eslami A, Akbarimehr D, Aflaki E, Hajitaheriha MM (2020) Geotechnical site characterization of the Lake Urmia super-soft sediments using laboratory and CPTu records. Mar Georesources Geotechnology 38:1223–1234. https://doi.org/10.1080/1064119X.2019.1672121

Feist SE, Hoque MA, Ahmed KM (2023) Coastal Salinity and Water Management Practices in the Bengal Delta: A Critical Analysis to Inform Salinisation Risk Management Strategies in Asian Deltas. Earth Syst Environ 7:171–187. https://doi.org/10.1007/s41748-022-00335-9

Ferdous J, Rahman MTU, Ghosh SK (2019) Derection of Total Dissolved Solids from Landsat 8 OLI Image in Coastal Bangladesh. ICCC 3:35–44. https://doi.org/10.17501/2513258X.2019.3103

Geopera T (2024) Sentinel-2 NDSI - Normalized difference salinity index. In: Geopera. https://docs.geopera.com/en/docs/spectral-indices/sentinel-2/ndsi. Accessed 3 Jan 2026

Gerardo R, De Lima IP (2022) Sentinel-2 satellite imagery-based assessment of soil salinity in irrigated rice fields in Portugal. Agriculture 12:1490. https://doi.org/10.3390/agriculture12091490

Gul I, Adil M, Lv F et al (2024) Microbial strategies for lead remediation in agricultural soils and wastewater: Mechanisms, applications, and future directions. Front Microbiol 15:1–16. https://doi.org/10.3389/fmicb.2024.1434921

Haq MI, Shamsudduha M, Zahid A et al (2024) What drives changes in surface water salinity in coastal Bangladesh? Front Water 6:1220540. https://doi.org/10.3389/frwa.2024.1220540

Hoque MA-A, Phinn S, Roelfsema C, Childs I (2016) Assessing tropical cyclone impacts using object-based moderate spatial resolution image analysis: a case study in Bangladesh. Int J Remote Sens 37:5320–5343. https://doi.org/10.1080/01431161.2016.1239286

Hossain H (2024) Cyclone Remal costs Khulna shrimp industry 323 C. In: Dhaka Tribune. https://www.dhakatribune.com/bangladesh/nation/348246/cyclone-remal-khulna-shrimp-industry-faces-323c. Accessed 25 June 2024

Hossen MA, Ayon MAG, Jubayer R (2025) Assessment of Tropical Cyclone Remal Induced Inundation in Patuakhali and Barguna Districts of Bangladesh Using Sentinel Satellite Images. Dhaka

Univ J Earth Env Sci 14:1–17. https://doi.org/10.3329/dujees.v14i1.83012
Islam K, Chowdhury S, Raja D (2015) Assessment of Ecological Change Due To Cyclone Using Remote Sensing Technique. JBIP 8:175–186
Islam K, Sarker S, Morsad G et al (2023) Spatial–temporal changes of shoreline and vegetation: impacts on mangrove cover along the Sundarbans area, Bangladesh. J Coast Conserv 28:10. https://doi.org/10.1007/s11852-023-01016-z
Jaman MH, Rafiq M, Rezwan N et al (2019) NDVI Based vegetation change detection of sundarbans due to the effect of cyvlone. Bulbul BUJSE 6:23–35
Kadam PM (2016) Study of pH and electrical conductivity of soil in Deulgaon Raja Taluka, Maharashtra. Int J Res Appl Sci Eng Technol (IJRASET) 4(4):399–402. https://www.cabidigitallibrary.org/doi/full/10.5555/20163194358
Kamran AA, Acharjee MR, Bhowmik P (2024) Assessment and mapping of soil salinity and groundwater quality in Nijhum Island, Hatiya Upazila, Noakhali. Discov Environ 2:64. https://doi.org/10.1007/s44274-024-00100-x
Khanam S, Haque MA, Hoque MF, Islam MT (2020) Assessment of salinity level and some nutrients in different depths of soil at Kalapara Upazila of Patuakhali District. ARRB 35:1–10. https://doi.org/10.9734/arrb/2020/v35i1230306
Konukcu F, Gowing JW, Rose DA (2006) Dry drainage: A sustainable solution to waterlogging and salinity problems in irrigation areas? Agric Water Manage 83:1–12. https://doi.org/10.1016/j.agwat.2005.09.003
Li X, Wu P, Delang CO et al (2021) Spatial-temporal variation, ecological risk, and source identification of nutrients and heavy metals in sediments in the peri-urban riverine system. Environ Sci Pollut Res 28:64739–64756. https://doi.org/10.1007/s11356-021-15601-y
Miah M, Mohammed F, Bhowmik S, Bottacharjee S (2024) Assessment of the coastal area water quality in Noakhali. Bangladesh IJSER 6:116–1123
Mukherjee N, Siddique G (2022) Soil, water salinization and its impact on household food insecurity in the Indian Sundarbans. In: Jana NC, Singh RB (eds) Climate, environment and disaster in developing countries. Springer Nature, Singapore, pp 217–233
Nadiruzzaman M, Paul BK (2013) Post-Sidr public housing assistance in Bangladesh: a case study. Environ Hazards 12:166–179. https://doi.org/10.1080/17477891.2012.759523
Nguyen K-A, Liou Y-A, Tran H-P et al (2020) Soil salinity assessment by using near-infrared channel and Vegetation Soil Salinity Index derived from Landsat 8 OLI data: a case study in the Tra Vinh Province, Mekong Delta, Vietnam. Prog Earth Planet Sci 7:1. https://doi.org/10.1186/s40645-019-0311-0
Prakash S, Varghese A, Amrutha AS, Baiju KR (2023) Assessment of Ecological Disturbance on Indian Sundarbans with Special Reference to Amphan Cyclone by Using Geospatial Technology. J Geospat Surv 3:26–32. https://doi.org/10.4038/jgs.v3i1.47
Rahman AZ, Shamsudduha M, Haq MI et al (2025) Soil and river-water salinity dynamics in coastal Bangladesh
Saha SK (2017) Cyclone, salinity intrusion and adaptation and coping measures in coastal Bangladesh. SACI 5:12–24. https://doi.org/10.20896/saci.v5i1.234
van Scheltinga CTHMT, Snethlage JS, Islam MF (2024) Water management to address salinity in agriculture in Bangladesh
Shapna KJ, Li J, Kabir MH et al (2024) Strengthening adaptation in coastal Bangladesh: community-based approaches for sustainable agriculture and water management. Dis Prev Res 3:1–28. https://doi.org/10.20517/dpr.2023.41
Shukurov S (2020) Soil Salinity Research and Mapping using Remote Sensing GIS. WJASS 5:1–3. https://doi.org/10.33552/WJASS.2020.05.000614
Sultan MT, Mahmud U, Khan MZ (2023) Addressing soil salinity for sustainable agriculture and food security: innovations and challenges in coastal regions of Bangladesh. Future Foods 8:100260. https://doi.org/10.1016/j.fufo.2023.100260
Sun J, Vecchi G, Soden B (2021) Sea Surface Salinity Response to Tropical Cyclones Based on Satellite Observations. Remote Sens 13:420. https://doi.org/10.3390/rs13030420
San Tsai C, Butler AP, Hoque MA (2020) Impact of tropical cyclone storm surges on groundwater salinity in southwest regions of Bangladesh. 19403. https://doi.org/10.5194/egusphere-egu2020-19403
Tsai C, Hoque MA, Vineis P et al (2024) Salinisation of drinking water ponds and groundwater in coastal Bangladesh linked to tropical cyclones. Sci Rep 14:5211. https://doi.org/10.1038/s41598-024-54446-6
San Tsai C, Mo H, Butler AP (2024) The effect of surge inundation on shallow groundwater salinity in the coastal low-lying poldered area of southwest Bangladesh-a 3D model investigation. p 7175
Uddin MR, Khandaker MU, Ahmed S et al (2024) Assessment of coastal river water quality in Bangladesh: implications for drinking and irrigation purposes. PLoS One 19:e0300878. https://doi.org/10.1371/journal.pone.0300878
Xu H, Yu R, Tang D et al (2020) Effects of tropical cyclones on sea surface salinity in the Bay of Bengal based on SMAP and Argo data. Water 12:2975. https://doi.org/10.3390/w12112975
Yang R, Huang J, Griffiths DV et al (2019) Optimal geotechnical site investigations for slope design. Comput Geotech 114:103111. https://doi.org/10.1016/j.compgeo.2019.103111